Title: Oral function improves interfacial integrity and sealing ability of conventional glass ionomer cements bonded to dentin.

Short title: Load improves sealing of ionomer cements-dentin interface.

Authors: Manuel Toledano[1*], Raquel Osorio[1], Inmaculada Cabello[1], Estrella Osorio[1], Manuel Toledano-Osorio[1], Fátima S. Aguilera[1].

Institution: [1]University of Granada, Faculty of Dentistry, Dental Materials Section.

Address: [1]University of Granada, Faculty of Dentistry, Dental Materials Section

   Colegio Máximo de Cartuja s/n

   18071 – Granada - Spain.

*Corresponding author: Prof. Manuel Toledano

   University of Granada, Faculty of Dentistry

   Dental Materials Section

   Colegio Máximo de Cartuja s/n

   18071 – Granada - Spain.

   Tel.: +34-958243788

   Fax: +34-958240809

   Email:toledano@ugr.es

Abstract

The aim was to investigate if load cycling affects interfacial integrity of glass-ionomer cements bonded to sound or caries-affected dentin. A conventional glass-ionomer, Ketac Bond and a resin-modified glass-ionomer, (Vitrebond Plus), were applied to dentin. Half of the specimens were load cycled. The interfaces were submitted to dye assisted confocal microscopy evaluation. The unloaded specimens of sound and carious dentin were deficiently hybridized when Ketac Bond was used. Ketac Bond samples showed an absorption layer and an adhesive layer that were scarcely affected by fluorescein penetration (nanoleakage), in sound dentin. Nevertheless, a higher degree of micropermeability was found in carious dentin. Load cycling improves sealing capability and remineralization at the cement-dentin interface, as porosity and nanoleakage diminished, in Ketac Bond specimens. In contrast, samples treated with Vitrebond Plus attained a rhodamine B-labeled absorption layer with scarce nanoleakage in both sound and carious unloaded dentin. The adhesive layer was affected by dye sorption throughout the porous cement-dentin interface. Samples treated with Vitrebond Plus had significant increases in nanoleakage and cement-dye sorption after load cycling. With the limitations of an *in vitro* study, it is expected that conventional glass-ionomers will provide major clinical efficacy when applied to carious-affected or sound dentin.

Keywords: Confocal, ionomers, dentin, remineralization, sealing.

INTRODUCTION

Glass ionomer cements (GICs) are used in preventive and restorative dental sciences to reestablish oral function to patients, thus making the analysis of dentin-material interfaces and their sealing ability a key concern (Grandfield & Engqvist, 2014). Conventional GICs are composed of fluoro-aluminosilicate glass (powder) and an aqueous solution of polyalkenoic acid, such as polyacrylic acid (liquid). Upon mixing and during the dissolution phase, multiple ions are released. Further, cross-linking between polyacid's carboxylic groups and ions are facilitated in the latest stage of gelation (Watson et al., 2014; Baig & Fleming, 2015). The previous application of an acid conditioner is mandatory, in order to demineralize the dentin substrate. This conditioning step exposes the micro-porous collagen fibrils network, where the cement is infiltrated (Shimada et al., 1999). Consequently, this shallow hybrid layer formed between the demineralized collagen (~1-2 μm depth) (Tay et al., 2004; Peumans et al., 2005) and the infiltrated cement contributes to micro and nano-mechanical bonding. The most important disadvantages of conventional GICs are their poor esthetic, lack of strength, toughness and wear resistance, decreased setting time, and moisture sensitivity. To offset these drawbacks, resin-modified glass ionomers (RMGIs) have been introduced (Coutinho et al., 2009). Chemical interaction is the primary bonding mechanism for RMGICs. Another bonding mechanism includes micro-mechanical interlocking into surface irregularities (Coutinho et al., 2007) thus, hybridizing dentin. RMGIs may not require previous conditioning. When RMGICs are applied without separate conditioners, micro-mechanical bonding is limited to the retention provided by intrinsic dentin surface roughness, and porosity created by RMGIC self-etching characteristics (Shimada et al., 1999). Not only are adequate restorative mechanical

properties in a cement needed, but the cement must also provide good sealing and remineralization capability for better clinical success rates amongst patients.

Dentin represents the most common dental substrate to be used in multiple adhesive techniques for restoration (De Munck et al., 2005). Sound dentin forms a three-dimensional matrix that is reinforced by mineral (apatite) (Bertassoni et al., 2009). Dentists must usually bond to irregular dentin substrates such as carious dentin. Caries-affected dentin consists of a partially demineralized substrate with a predominantly intact collagen matrix. This matrix should be preserved during clinical treatment because it serves as a suitable substrate for dentin adhesion and can be remineralized. Caries-affected dentin typically exhibits a higher degree of porosity which is commonly associated with a partial lack of minerals around and within the collagen fibrils. Hypo-mineralized and porous caries-affected dentin substrate may allow for a deeper penetration of the cement (Wang et al., 2007). Thus, a much thicker hybrid layer is created over the non-infiltrated demineralized collagen zone of the substratum which is located at the bottom of the hybrid layer. This unprotected collagen may become a site for the non-bacterial degradation of collagen, and should be preserved for potential remineralization (Wang & Spencer 2003; Osorio et al., 2011). Restored teeth are constantly subjected to challenges caused by the cyclical stresses from mastication and para-functional habits. This occlusal stress may cause mechanical and chemical degradation within the dentin interfaces (Nikaido et al., 2002; Osorio et al., 2005). However, mechanical loading has also been shown to induce, in some cases, dentin remineralization (Toledano et al., 2013a).

In order to determine nanoleakage, degradation and remineralization, studies on interfacial porosity and micropermeability should be performed. Adequate cement-dentin sealing is necessary for the successful dental restoration. One of the least

invasive and destructive methods of studying the morphology of the interface between the glass ionomer cement and the dentin structure may be carried out with the use of the fluorescent confocal optical microscope (Sidhu & Watson, 1995). Confocal laser scanning microscopy (CLSM) is capable of individually exciting different fluorochromes by applying selective wavelengths (Griffiths et al., 1999). Fluorescent markers can be incorporated into the cement prior to their application. This technique allows for the observation of the hybrid layer morphology to be formed in thin optical sections, with the added advantage of needing only minimal preparation of each sample. CLSM also permits the visualization of resin tag extensions, the measurement of the adhesive layer thickness, and the assessment of possible defects or alterations at the bonded restoration interface (D'Alpino et al., 2006; De Oliveira et al., 2010). The micropermeability test serves to evaluate fluid interactions at the interface and also the sealing ability of the adhesive cement (Sidhu & Watson, 1998). Nanoleakage strongly suggests possible pathways for permeability through the porous hybrid zone itself. Nanoleakage typically occurs in the absence of gaps through nanometer-sized spaces of approximately 0.02 µm, and starts at the bottom of the hybrid layer, where the resin monomers were not infiltrated. (D'Alpino et al., 2006). Its clinical significance is unknown, but interfacial failures may occur if the fluid is allowed to penetrate the interface and cause degradation of demineralized collagen fibers and adhesive monomers (Griffiths et al., 1999). Recently, a new method to assess dentin remineralization, based on the use of a calcium-chelator fluorophore, has been proposed (Profeta et al., 2013). The aim of this study was to analyze the morphology and the micropermeability of sound and caries-affected dentin surfaces treated with both a conventional glass ionomer and a resin-modified glass ionomer cement, after *in vitro*

mechanical loading stimuli. The null hypothesis is that mechanical loading and type of GIC do not influence nanoleakage and mineral precipitation.

MATERIAL AND METHODS

Specimen preparation, bonding procedures and mechanical loading

Twenty four human third molars (twelve sound specimens and twelve with occlusal caries) were obtained with informed consent from donors (20–40 years of age), under the protocol approved by the Institution Review Board. Molars were stored at 4ºC in 0.5% chloramine T for up to 1 month before use. A flat mid-coronal sound or carious dentin surface was exposed using a hard tissue microtome (Accutom-50; Struers, Copenhagem, Denmark) equipped with a slow-speed, water-cooled diamond wafering saw (330-CA RS-70300, Struers, Copenhagen, Denmark). The inclusion criteria for carious teeth were that the caries lesion, surrounded by sound dentin, should be limited to the occlusal surface and that it extended at least half the distance from the enamel-dentin junction to the pulp chamber. To obtain caries-affected dentin, grinding was performed by using the combined criteria of visual examination, surface hardness using a dental explorer, and staining with the aid of a caries detector solution (CDS, Kuraray Co., Ltd., Osaka, Japan). Using this procedure all soft, stainable, carious dentin was removed. The caries-affected non-stained dentin which was relatively hard was left on the experimental side. One180-grit silicon carbide (SiC) abrasive paper was mounted on a water-cooled polishing machine (LaboPol-4, Struers, Copenhagem, Denmark) and was used to produce a clinically relevant smear layer (Koibuchi et al., 2001). The conventional glass ionomer cement, Ketac-Bond (3M Deustchland GmbH, Neuss, Germany) and the resin-modified glass ionomer cement, Vitrebond Plus (3M Deustchland GmbH, Neuss, Germany) were tested. The chemical components and

descriptions of the materials are provided in Table 1. Glass ionomer cements were later applied to sound and caries-affected teeth following the manufacturer´s instructions, and a flowable resin composite (X-FlowTM, Dentsply, Caulk, UK) was placed incrementally in five 1 mm layers and light-cured with a Translux EC halogen unit (Kulzer GmbH, Bereich Dental, Wehrheim, Germany) for 40 s. Half of the teeth were then stored for 24 h in a simulated body fluid solution (SBF) (International Organization for Standardization, 2012), and the other half were submitted to mechanical loading, in a SBF solution (100,000 cycles, 3 Hz, 49 N) (S-MMT-250NB; Shimadzu, Tokyo, Japan) (Toledano et al., 2014a). The load cycling lasted for 9 hours and 15 minutes. For the rest of the time, the remainder of the 24 hours, the loaded specimens were kept in SBF solution, at 37 ºC. The case table (Table 2) refers to the group classification.

Confocal microscopy evaluation

Previous to the cement application, glass ionomers were doped with 0.05 wt% Rhodamine-B (RhB: Sigma-Aldrich Chemie Gmbh, Riedstr, Germany). In 6 samples of sound dentin and 6 samples of caries-affected dentin, the pulpal chamber was filled with 1 wt% aqueous/ethanol fluorescein (Sigma-Aldrich Chemie Gmbh, Riedstr, Germany) for 3 h (Toledano et al., 2014a, 2014b). The rest of the molars were immersed in 0.5 wt% xylenol orange solution (XO: Sigma-Aldrich Chemie Gmbh, Riedstr, Germany), excited at 514-nm for 24 h at 37 ºC (pH 7.2). Specimens were copiously rinsed with water and treated in an ultrasonic water bath for 2 min. The specimens were cut in resin-dentin slabs and polished using ascending grit SiC abrasive papers (#1200 to #4000) on a water-cooled polishing device (Buehler-MetaDi, Buehler Ltd. Lake Bluff, IL, USA). A final ultrasonic cleaning (5 min) concluded the specimen preparation. Analysis of the bonded interfaces were performed by dye assisted by a confocal microscopy evaluation

(CLSM), and attained by using a confocal laser scanning microscope (SP5 Leica, Heidelberg, Germany) equipped with a 20x, 40x and 60x oil immersion lenses. The fluorescein dye used in the confocal microscopy evaluation was activated by blue light (488-495 nm) and emited yellow/green (520 nm), while the ultramorphology evaluation (cement-diffusion) was executed using a Rhodamine excitation laser. The rhodamine was excited using a green light (540 nm) and emited red in color (590 nm). Applying this method, CLSM images were obtained with a 1 μm z-step to optically section the specimens to a depth of up to 12-10 μm below the surface. The interface surface z-axis scans were then arbitrarily pseudo-colored by the same operator for better exposure and compiled into single projections using Leica image-processing software SP2 (Leica, Heidelberg, Germany). The resolution of the CLSM images was 1024 x 1024 pixels. Five optical images were randomly captured from each resin-dentin interface, and micrographs representing the most common features of nanoleakage were obtained along the bonded interfaces and later selected (Profeta et al., 2013; Toledano et al., 2013b). Some fluorescences were separated into spectral regions while others were not, allowing the operator to have full regional control of the light spectrum directed to each respective laser emission channel.

RESULTS

Figures 1 to 16 show the CLSM cement-dentin interface images obtained in the experimental groups.

CLSM analysis revealed that the Ketac Bond cement-sound dentin interfaces were hybridized in both unloaded (Fig. 1) and load cycled (Fig. 3) specimens. Microstructures colored in red represent the rhodamine B-labeled cement location. The multifluorescence examination showed that the cement layer was completely affected

by fluorescein penetration (*i.e.* micropermeability) and water sorption, traced in green and yellow, through the porous cement-dentin interface. Ketac Bond cement was able to diffuse within the porous dentin, in both types of unloaded and loaded dentin, creating thick hybrid layers (Figs. 1A/C, 3A/C), though remineralization occurred at the cement-dentin interface (Figs. 1D, 2A/C). Funneled dentinal tubules were found, more often in the unloaded specimens (Fig. 1A). Rhodamine B, penetrated along the tubules through the hybrid zone, thus characterizing the interface with the presence of multiple cement tags (Fig. 1C). Discontinuities in the tubular filling with Ketac Bond were seen in the single labeled sample (Fig. 1C). Mechanical loading produced weak outlined fluorescence due to faint Ca-minerals deposited within the bonding interface and inside the dentinal tubules. This was observed when treating the load cycled sound specimens, with xylenol (Xo-dye) (Figs. 4A/C).

Ketac Bond cement-carious dentin interfaces were deficiently hybridized in the unloaded specimens (Fig. 5). A tight dye sorption throughout the thickness of the hybrid layer evidenced the lack of sealing found within these unloaded interfaces (Fig. 5B). New mineral deposits appeared at the cement-carious dentin interface, confirmed by the moderate reflective (Fig. 5D) and fluorescent (Figs. 6A/C) signals. When Ketac Bond cement-carious dentin interfaces were load cycled, less nanoleakage and water sorption were detected, though a very limited amount of dye diffused into the adhesive cement layer (Fig. 7A). After applying load cycling, a moderate reflective signal was observed from inside the dentinal tubules (Fig. 7D) thus, indicating the presence of mineral components. A clear fluorescence signal within the hybrid layer was recorded and both dentin tubules wall and cement tags were identified with only a calcium-chelator Xo-dye (Fig. 8C).

After CLSM analysis, it was observed that the Vitrebond Plus cement-sound dentin interfaces were moderately hybridized in both unloaded (Fig. 9) and load cycled (Fig. 11) specimens. The unloaded specimens showed minimal water sorption, and a light spectral overlap (yellow) within the body of the cement. A faint remineralization zone was observed when the interface was analyzed with the fluorescent calcium-chelator dye Xo (Fig. 10C). The hybrid layer showed any nanoleakage signal. Load cycling produced evident signs of nanoleakage at the hybrid layer and strong dye sorption throughout the entire thickness of the cement (Figs. 11A/B). Similarly, RMGIC interfaces achieved with Vitrebond Plus evidenced strong reflective signal (Fig. 11D) and so presence of xylenol-stained Ca-deposits at the walls of dentinal tubules and within the cement tags (Figs. 12 A/C).

Both micropermeability and water sorption were not present in the unloaded specimens of Vitrebond Plus bonded to caries-affected dentin, though the partially demineralized peritubular and intertubular dentin, affected by the carious process, was remineralized (Figs. 13, 14). Load cycling produced severe dye sorption throughout the thickness of the cement layer (Fig. 15), strong micropermeability within dentinal tubules and evident nanoleakage signals at the hybrid layer. Remineralization was evidenced at the interface, as both intertubular and peritubular dentin showed deposits of new apatite (Fig. 16).

Vitrebond Plus attained less sealing capability than Ketac Bond, as a stronger yellowish spectral overlap was determined in the specimens treated with Vitrebond Plus, especially after mechanical loading (Figs. 11, 15).

DISCUSSION

Results confirm that conventional glass ionomer cements allowed for improved interfacial integrity and sealing ability in, especially, caries-affected dentin. Conventional glass-ionomer cement was compared to the performance of resin-modified glass-ionomer cement. Nanoleakage, micropermeability and dye sorption were almost absent in this group, especially after load cycling.

In this study, the adhesive potential and sealing capability of these two glass ionomer-based cements applied to sound and caries-affected dentin substrata have been investigated. The null hypothesis had to be partially rejected, as mechanical loading and type of GIC do not influence nanoleakage and mineral precipitation.

The sealing ability of the conventional GIC, Ketac Bond

The Ketac Bond-sound dentin interfaces, though hybridized, presented some deficiencies in both intertubular and peritubular dentin (Figs. 1, 3). After conducting a multi-fluorescence examination, it was observed the presence of micropermeability and water sorption. Both demonstrated the lack of intimate interaction within the hydroxyapatite-coated collagen. The movement of the fluorescent dye into the cement material indicates the micropermeability of the dentin interface and it also confirms the presence of a highly stained unsealed area adjacent to the dentin interface (Sidhu & Watson, 1998). This might lead to the instability of the interface in the long term (Shafiei et al., 2015). Samples were labeled simultaneously, by combining specific filters. The specimens matched the excitation line and the emission band. This technique allows for the assessment of samples that contain two fluorophores with different target labels, thus permitting each target to be observed separately, or at the same time. The advantage of simultaneous excitation is that the corresponding pixels

from the two images are definitely in register. A single spot of incident light can be observed as the source of both images (Pawley, 2006), allowing the overlapping between the two original channels. In addition, a submicron hybrid layer, in which hydroxyapatite remained attached to collagen (Coutinho et al., 2007) was noted to improve the chemical and micromechanical bonding of the ionomeric cement. The polyacrylic acid conditioner serves to partially remove the smear layer without the complete removal of the calcium ions available for chemical bonding and remineralization.

Confocal microscopy observations reflected preparations of the dentin surface with funneling of the tubular orifices and well defined lateral tubules which also contributed to migration of rhodamine around the main tags and the rest of the interface. Funneling occurred more frequently in the unloaded specimens (Fig. 1A). It is considered an essential sign of degradation of poor adhesive cement infiltration within demineralized peritubular dentin (Profeta et al., 2013). The green-colored dye, placed in the pulp chamber allowed to diffuse toward the red-colored hybrid layer, showing spectral overlap (yellow) in the emission profile of these two dyes. This moderate degree of degradation may be attributed to the high hydrophilicity of this interface. These conditions may have permitted excessive water sorption and induced discrete interface degradation. Discontinuities observed in the tubular filling with Ketac Bond were also seen in the single labeled sample (Fig. 1C), thus indicating the intermittent passage of fluorescein through all possible routes to the restorative interface and within the cement. The fluorophore cement-dentin interface permeability was evidenced by the dye movement (lability) which occurred from the dentin to the restoration interface and also within the cement (Sidhu & Watson, 1998). Nevertheless, mechanical loading of sound samples permitted to observe, with xylenol (Xo-dye) (Figs. 4A, 4C), weak

outlined fluorescence due to faint Ca-minerals deposited within the bonding interface and inside the dentinal tubules. These findings may be interpreted as dentin remineralization (Toledano et al., 2015). The Xo-dye is commonly employed in bone remineralization studies due to its ability to form complexes with divalent calcium ions (Rahn & Perren, 1971; Profeta et al, 2013).

GICs have been primarily studied as the restorative material of choice for the remineralization of caries-affected dentin (Aykut-Yetkiner et al., 2014). Ketac Bond cement-carious dentin interfaces were deficiently hybridized when mechanical stimuli was not applied (Fig. 5). This phenomenon represents a risk of future potential degradation (Osorio et al., 2011), and communication with biofilm (Aykut-Yetkiner et al., 2014). Despite this potential risk, dentin tubules were found to become narrower with the presence of mineralized precipitates composed of apatite aggregates at their entrance. Nevertheless, these interfaces were found to be more efficiently hybridized after load cycling (Fig. 7), as new mineral deposited at the cement-carious dentin interface (Figs. 6A, 6C). The new minerals were represented as regions in orange (xylenol solution). These mineralization contributed to a lower nanoleakage and water sorption, though some dye diffusion still remained into the cement (Fig. 7A). The new mineral aggregates were observed at the hybrid layer, at the dentinal walls and in the cement tags (Figs. 7D, 8C). These nano-aggregates are thought to form flowable nano-precursors which can precipitate as polyelectrolyte-stabilized apatite nano-crystals (Tay & Pashley, 2008). The Ca-deposits precipitation is guided by a polyphosphate molecule which acts as an apatite template, hence encouraging crystalline alignment, leading to hierarchical dentin remineralization (Liu et al., 2011). On the contrary, sound dentin did not show any potential site for functional remineralization. This was attributed to the fact that the GIC requires preexistent nucleation sites, as in partially demineralized

dentin (caries-affected dentin). As a result, the local bioactivity of conventional GICs after *in vitro* load cycling can produce functional mineralization at the interface, within the underlying dentin substrate. Moreover, the pressure gradient from mechanical loading increases the interstitial fluid (McAllister and Frangos, 1999) towards the restorative interface, where the glass ionomer cement, with high values of water sorption, is present. As a result, some balance between sorption and solubility phenomena occurs. This leads to the formation of a silica gel at the particle peripheries that links the filler core to the matrix phase, hence supporting the hypothesis that 'self-healing' or 'repair' could be possible with the application of glass ionomer cements (Davidson, 1994; Toledano et al., 2003) and in this way improve the interface seal. The advantage of this for the minimally invasive management of caries-affected dentin is self-evident.

The sealing ability of the resin-modified GIC, Vitrebond Plus

Cement-sound dentin hybridization was moderately achieved in both unloaded (Fig. 9) and load cycled (Fig. 11) specimens, when Vitrebond Plus was used. This can be due to the resin and polyalkenoic acid mixture (Coutinho et al., 2007) found within its chemical formulation. Vitrebond Plus, in the unloaded group, made direct contact with the apparently hybridized dentin throughout the multilocular phase (Tay et al., 2004) without any sign of unprotected collagen at the interface (Fig. 9A), nor any presence of cement tags (Fig. 9 B). Both findings suggest the absent of nanoleakage (no green or yellow zones at the hybrid layer) and cement infiltration within the dentinal tubules (no red coloration within the tubules). This finding was attributable to the rapid initial set via RMGIC light-curing (Sidhu & Watson, 1998). Load cycling was observed to deteriorate the cement-dentin interface, as evidenced by signs of nanoleakage at the

hybrid layer and strong dye sorption within the cement (Figs. 11A/B). Contrary to the assertion supported by Sidhu et al (2002), it is clear that the RMGIC hybrid layer has not acted as stress-breaking layer. The strong and superficial mechanical interlocking might be responsible for this finding, which possibly can be a consequence of the lack of a previous conditioning step (Coutinho et al., 2009). Shafiei et al. (2015) have stated that one of the disadvantages of RMGICs is their degradability which may deteriorate faster than conventional GICs. Nevertheless in this study, RMGIC interfaces were also characterized by a strong reflective signal, in white (Fig. 11D), and a richly dye-infiltrated band which was flooded by fluorophores leaching from the cement (Figs. 11A/C). Moreover, a consistent presence of xylenol-stained Ca-deposits, in orange, at the walls of dentinal tubules and within the cement tags was also observed (Figs. 12A/C).

Nevertheless, Vitrebond Plus applied in carious dentin was found to preserve interface integrity, as both micropermeability and water sorption were not present in the unloaded specimens (Figs. 13 A/B), confirming sealing ability. This cement, as in the sound dentin (Fig. 9), achieved a close and irregular contact with dental substrate. Minimal demineralization of the dentin surface was created (Coutinho et al., 2007) due to its self-etching characteristics (Shimada et al., 1999). This partially demineralized peritubular and intertubular dentin, affected by the carious process, was remineralized after Vitrebond Plus application (Fig. 14). In contrast, after load cycling the Vitrebond Plus application was found to be less effective. The results from the Vitrebond Plus application showed strong micropermeability within dentinal tubules and evident nanoleakage signals at the hybrid layer. This was demonstrated by the observance of severe dye sorption throughout the thickness of the cement layer (Fig. 15), reflected as extended yellow areas in the cement location. Deeper cement-labelling fluorophore

infiltration into the higher mineralized peritubular and intertubular dentin (Fig. 15 C) is associated with lateral diffusion of dye permeating from the pulp space through to the demineralized dentin in that area. This consequently led to the mixing of both dyes (Fig. 15A). The loading stress which is concentrated mostly at the interface between the adhesive cement and the roughly 2 μm thick hybrid layer (Tay et al., 2004) and within the hybrid layer (Nikaido et al., 2002; Toledano et al., 2006), may have accelerated resin-dentin interface degradation (Fig. 15A). In spite of these findings, remineralization was evidenced at the cement-dentin interface, as both intertubular and peritubular dentin were stained in orange with fluorescent calcium-chelator Xo-dye (Fig. 16 C), due to the hydroxyapatite formation (Atmeh et al., 2012).

The sealing ability of Ketac Bond (conventional GIC) *vs* Vitrebond Plus (RMGIC)

Despite the evolution of GICs, several studies have demonstrated that none of these materials have complete marginal sealing capability, which is considered as one of the primary reasons for microleakage (Doozandeh et al., 2015) and further damage of the interface. In general, Vitrebond Plus showed a stronger yellowish spectral overlap than Ketac Bond in the profile emission both dyes (red and green) (Figs 11, 3) after mechanical loading. The poorer sealing performance results of Vitrebond Plus when compared to Ketac Bond can be attributed to a number of factors. One of the factors is the swelling of the resin component of the Vitrebond Plus, driven by the chemical behavior of its solvent system (Nicholson, 1998) HEMA (a water-soluble monomer), which absorbs water (Sidhu & Watson, 1998). Because of its chemical characteristics, HEMA damages the polyacrylic acid molecule structures and, tends to favor the phase-separation of components (Nicholson, 1998). On the other hand, this phenomenon doesn´t occur with the application of Ketac Bond, a conventional glass ionomer cement,

where no resin component is present. In contrast, with the application of Vitrebond Plus the release of its resin components is linked to evident signs of nanoleakage (Fig. 11) due to the increase of water uptake throughout the thickness of the adhesive cement. The yellow overlapped light spectra found when Ketac Bond was used, was probably caused by the existence of a partially demineralized layer both found at the bottom of the absorption layer, and below the hybrid layer (Coutinho et al., 2007). Another possible cause for the poor sealing performance of Vitrebond when compared to Ketac bond may has been the presence of the smear layer, which may also have interfered with the infiltration of the material to the underlying dental surface, hence reducing the effect of complete hybridization (Tay et al., 2004). The superior performance of Ketac Bond on the other hand, can be explained by the presence of calcium-polycarboxylate salts deposited in the partially exposed dentinal collagen. This, in turn, resulted in a reaction between the polyalkenoic acid and calcium extracted from the dentin, enhanced sealing and represents the gel phase. Solely the application of conditioner on dentin by the polyalkenoic acid may induce formation of a hybrid layer and a gel phase (Coutinho et al., 2007). Whereas, Vitrebond Plus lacks this pretreatment, thus canceling the possibility of an active mechanical adhesion procedure without impairing its adhesive performance. Nevertheless, the results of this study suggest that chemical interaction based on ionic bond formation is the primary bonding mechanism for Vitrebond Plus copolymer to dentin.

With regards to the effect of load cycling application on the presence of carious dentin, a wide range of growth factors and matrix signaling molecules can be released or activated within the dentin. These conditions allow for remodeling and thus contribute to further tissue genesis and regeneration. It has been demonstrated that intermittent compressive load stimulates the proteic synthesis in osteocytes and alkaline

phosphatase activity in osteoblasts both *in vivo* and *in vitro* conditions. Alkaline phosphatase, present at all mineralization sites, hydrolyzes phosphate esters producing free phosphate, and thus apatite supersaturation (Posner et al., 1986). The new mineral deposits that extended along the whole interface were observed after using the fluorescent calcium-chelator dye Xo, and appeared in orange when both CICs were used (Figs 4, 6, 8, 12, 16). These nucleated minerals can be interpreted as a natural defense mechanism against caries attack and serve the purpose of preventing toxins, acids and cariogenic bacteria from penetrating deeper into a tooth and reaching its pulp (Zavgorodniy et al., 2008). It may be further speculated that, through mechanical stimuli, an enhanced sealing capability of carious dentin can be achieved. Furthermore, stimuli, injury and trauma can easily augment the pulpal hydrostatic pressure of the dentin structure. This pressure gradient (14-70 cm H_2O) from mechanical loading increases interstitial fluid (McAllister & Frangos, 1999). This fluid flow, has been shown to have an important role in load-induced hard-tissue remodeling.

To the best of our knowledge, this is the first study that evaluates the sealing capability, by CLSM characterization, of glass ionomer cement-dentin on a sound and a caries-affected interface that has been submitted to load cycling. Both anecdotal and scientific evidence confirm that glass-ionomer cement is able to bring about the remineralization of partly demineralized dentin and are of highly valued by professionals in the field as the preferred approach in the management of caries lesions. However, if the circumstances which result in the remineralization of demineralized dentin by a glass ionomer cement do not favor the complete sealing of the interface, then the risk of interface degradation and further pulp damage will compromise the restorative management of caries. At present, further work is needed to provide a more detailed understanding of how and why dentin remineralization may vary with mechanical

loading and thermocycling with the use these smart restorative materials. Additional further research is also warranted to find out how the observed modifications correlate with the temporal or spatial healing distribution. Moreover, the maturation processes in dentin remineralization events also need to be investigated. Despite having good potential, the undertaking of further clinical studies are also recommended to confirm the bonding effectiveness and the better overall performance of conventional glass ionomer cements and their application as restorative materials in dentistry.

CONCLUSIONS

1. The conventional glass ionomer cement (Ketac Bond) attained higher sealing ability in cement-dentin interfaces than the resin-modified glass ionomer cement (Vitrebond Plus). Nanoleakage assessments denoted lower pathways for micropermeability with Ketac Bond than with Vitrebond Plus in both sound and caries-affected dentin. With Ketac Bond, polyacrylic acid conditioning produced dentin hybridization, superior nucleation and mineralization over the outcomes achieved with Vitrebond Plus. These results led to an enhanced sealing capacity at the cement-dentin interface, thus demonstrating Ketac Bond superior effectiveness over that of Vitrebond Plus.

2. Load cycling promoted less micropermeability when the conventional glass ionomer cement (Ketac Bond) was used in sound dentin, and this effect became even more pronounced in the case of caries-affected dentin. Both interfacial integrity and stability are largely expected to increase in carious dentin after mechanical loading.

3. Mechanical cycling induced higher micropermeability and water sorption within the hybrid layer when the resin-modified glass ionomer cement (Vitrebond Plus) was used in sound dentin. Nanoleakage and dye sorption were even more evident in

case of caries-affected dentin. The loading stress concentration on the mechanical interlocking surface between the cement and the non-conditioned dentin surface accelerated bonded interface degradation.

REFERENCES

ATMEH, A.R., CHONG, E.Z., RICHARD, G., FESTY, F. & WATSON, T.F. (2012). Dentin-cement interfacial interaction: calcium silicates and polyalkenoates. *J Dent Res* **91**, 454-459.

AYKUT-YETKINER, A., SIMŞEK, D., ERONAT, C. & CIFTÇIOĞLU, M. (2014). Comparison of the remineralisation effect of a glass ionomer cement versus a resin composite on dentin of primary teeth. *Eur J Paediatr Dent* **15**, 119-121.

BAIG, M.S. & FLEMING, G.J. (2015). Conventional glass-ionomer materials: A review of the developments in glass powder, polyacid liquid and the strategies of reinforcement. *J Dent* **43**, 897-912.

BERTASSONI, L.E., HABELITZ, S., KINNEY, J.H., MARSHALL, S.J. & MARSHALL, G.W. JR. (2009). Biomechanical perspective on the remineralization of dentin. *Caries Res* **43**, 70-77.

COUTINHO, E., YOSHIDA, Y., INOUE, S., FUKUDA, R., SNAUWAERT, J., NAKAYAMA, Y., DE MUNCK, J., LAMBRECHTS, P., SUZUKI, K. & VAN MEERBEEK, B. (2007). Gel phase formation at resin-modified glass-ionomer/tooth interfaces. *J Dent Res* **86**, 656-661.

COUTINHO, E., CARDOSO, M.V., DE MUNCK, J., NEVES, A.A., VAN LANDUYT, K.L., POITEVIN, A., PEUMANS, M., LAMBRECHTS, P. & VAN MEERBEEK, B. (2009). Bonding effectiveness and interfacial characterization of a nano-filled resin-modified glass-ionomer. *Dent Mater* **25**, 1347-1357.

D'ALPINO, P.H., PEREIRA, J.C., SVIZERO, N.R., RUEGGEBERG, F.A. & PASHLEY, D.H. (2006). Factors affecting use of fluorescent agents in identification of resin-based polymers. *J Adhes Dent* **8**, 285-292.

DAVIDSON, C.L. (1994). Glass-ionomer bases under posterior composites. *J Esthet Dent* **6**, 223-226.

DE MUNCK, J., VAN LANDUYT, K., PEUMANS, M., POITEVIN, A., LAMBRECHTS, P., BRAEM, M. & VAN MEERBEEK, B. (2005). A critical review of the durability of adhesion to tooth tissue: methods and results. *J Dent Res* **84**, 118-132.

DE OLIVEIRA, M.T., ARRAIS, C.A., ARANHA, A.C., EDUARDO, C. DE PAULA, MIYAKE, K., RUEGGEBERG, F.A. & GIANNINI, M. (2010). Micromorphology of resin-dentin interfaces using one-bottle etch&rinse and self-etching adhesive systems on laser-treated dentin surfaces: a confocal laser scanning microscope analysis. *Lasers Surg Med* **42**, 662-670.

DOOZANDEH, M., SHAFIEI, F. & ALAVI, M. (2015). Microleakage of Three Types of Glass Ionomer Cement restorations: Effect of CPP-ACP Paste Tooth Pretreatment. *J Dent (Shiraz)* **16**, 182-188.

GRANDFIELD, K. & ENGQVIST, H. (2014). Characterization of dental interfaces with electron tomography. *Biointerphases* **9**, 29001.

GRIFFITHS, B.M., WATSON, T.F. & SHERRIFF, M. (1999). The influence of dentine bonding systems and their handling characteristics on the morphology and micropermeability of the dentine adhesive interface. *J Dent* **27**, 63-71.

INTERNATIONAL ORGANIZATION FOR STANDARDIZATION. (2012). ISO 23317. Implants for surgery - In vitro evaluation for apatite-forming ability of implant materials. Geneva, Switzerland: International Organization for Standardization.

KOIBUCHI, H., YASUDA, N. & NAKABAYASHI, N. (2001). Bonding to dentin with a self-etching primer: the effect of smear layers. *Dent Mater* **17**, 122-126.

LIU, Y., KIM, Y.K., DAI, L., LI, N., KHAN, S.O., PASHLEY, D.H. & TAY, F.R. (2011). Hierarchical and non-hierarchical mineralisation of collagen. *Biomaterials* **32**, 1291-1300.

MCALLISTER, T.N. & FRANGOS, J.A. (1999). Steady and transient fluid shear stress stimulate NO release in osteoblasts through distinct biochemical pathways. *J Bone Miner Res* **14**, 930-936.

NICHOLSON, J.W. (1998). Chemistry of glass-ionomer cements: a review. *Biomaterials*. **19**, 485-494.

NIKAIDO, T., KUNZELMANN, K.H., CHEN, H., OGATA, M., HARADA, N., YAMAGUCHI, S., COX, C.F., HICKEL, R. & TAGAMI, J. (2002). Evaluation of thermal cycling and mechanical loading on bond strength of a self-etching primer system to dentin. *Dent Mater* **18**, 269-275.

OSORIO R., TOLEDANO M., OSORIO E., AGUILERA F.S. & TAY F.R. (2005). Effect of load cycling and in vitro degradation on resin-dentin bonds using a self-etching primer. *J Biomed Mater Res A* **15**, 399-408.

OSORIO, R., YAMAUTI, M., OSORIO, E., ROMÁN, J.S. & TOLEDANO, M. (2011). Zinc-doped dentin adhesive for collagen protection at the hybrid layer. *Eur J Oral Sci* **119**, 401-410.

PAWLEY J.B. (2006). *Handbook of Biological Confocal Microscopy,* third ed. New York, USA: Springer.

PEUMANS, M., KANUMILLI, P., DE MUNCK, J., VAN LANDUYT, K., LAMBRECHTS, P. & VAN MEERBEEK, B. (2005). Clinical effectiveness of contemporary adhesives: a systematic review of current clinical trials. *Dent Mater* **21**, 864-881.

POSNER, A.S., BLUMENTHAL, N.C. & BOSKEY, A.L. (1986). Model of aluminum-induced osteomalacia: inhibition of apatite formation and growth. *Kidney Int* **18**, S17-S19.

PROFETA, A.C, MANNOCCI, F., FOXTON, R., WATSON, T.F., FEITOSA, V.P., DE CARLO, B., MONGIORGI, R., VALDRÉ, G. & SAURO, S. (2013). Experimental etch-and-rinse adhesives doped with bioactive calcium silicate-based micro-fillers to generate therapeutic resin-dentin interfaces. *Dent Mater* **29**, 729-741.

RAHN, B.A. & PERREN, S.M. (1971). Xylenol orange, a fluorochrome useful in polychrome sequential labeling of calcifying tissues. *Stain Technol* **46**, 125-129.

SHAFIEI, F., AKBARIAN, S. & KARIM ETMINAN, M. (2015). Effect of Adhesive Pretreatments on Marginal Sealing of Aged Nano-ionomer Restorations. *J Dent Res Dent Clin Dent Prospects* **9**, 144-150.

SHIMADA, Y., KONDO, Y., INOKOSHI, S., TAGAMI, J. & ANTONUCCI, J.M. (1999). Demineralizing effect of dental cements on human dentin. *Quintessence Int* **30**, 267-273.

SIDHU, S.K., PILECKI, P., CHENG, P.C. & WATSON, T.F. (2002). The morphology and stability of resin-modified glass-ionomer adhesive at the dentin/resin-based composite interface. *Am J Dent* **15**, 129-136.

SIDHU, S.K. & WATSON, T.F. (1995). Resin-modified glass-ionomer materials. Part 1: Properties. *Dent Update* **22**, 429-432.

SIDHU, S.K. & WATSON, T.F. (1998). Interfacial characteristics of resin-modified glass-ionomer materials: a study on fluid permeability using confocal fluorescence microscopy. *J Dent Res* **77**, 1749-1759.

TAY, F.R. & PASHLEY, D.H. (2008). Guided tissue remineralisation of partially demineralised human dentine. *Biomaterials* **29**, 1127-1137.

TAY, F.R., SIDHU, S.K., WATSON, T.F. & PASHLEY, D.H. (2004). Water-dependent interfacial transition zone in resin-modified glass-ionomer cement/dentin interfaces. *J Dent Res* **83**, 644-649.

TOLEDANO, M., OSORIO, R., OSORIO, E., FUENTES, V., PRATI, C. & GARCIA-GODOY, F. (2003). Sorption and solubility of resin-based restorative dental materials. *J Dent* **31**, 43-50.

TOLEDANO, M., OSORIO, R., ALBALADEJO, A., AGUILERA, F.S., TAY, F.R. & FERRARI, M. (2006). Effect of cyclic loading on the microtensile bond strengths of total-etch and self-etch adhesives. *Oper Dent* **31**, 25-32.

TOLEDANO, M., AGUILERA, F.S., YAMAUTI, M., RUIZ-REQUENA, M.E. & OSORIO, R. (2013*a*). In vitro load-induced dentin collagen-stabilization against MMPs degradation. *J Mech Behav Biomed Mater* **27**, 10-18.

TOLEDANO, M., SAURO, S., CABELLO, I., WATSON, T. & OSORIO, R. (2013*b*). A Zn-doped etch-and-rinse adhesive may improve the mechanical properties and the integrity at the bonded-dentin interface. *Dent Mater* **29**, e142-e152.

TOLEDANO, M., AGUILERA, F.S., SAURO, S., CABELLO, I., OSORIO, E. & OSORIO, R. (2014*a*). Load cycling enhances bioactivity at the resin-dentin interface. Dent Mater **30**, e169-e188.

TOLEDANO, M., OSORIO, E., AGUILERA, F.S., SAURO, S., CABELLO, I. & OSORIO, R. (2014*b*). In vitro mechanical stimulation promoted remineralization at the resin/dentin interface. *J Mech Behav Biomed Mater* **30**, 61-74.

TOLEDANO, M., CABELLO, I., AGUILERA, F.S., OSORIO, E., TOLEDANO-OSORIO, M. & OSORIO, R. (2015). Improved sealing and remineralization at the resin-dentin interface after phosphoric acid etching and load cycling. *Microsc Microanal* **21**, 1530-1548.

WANG, Y. & SPENCER, P. (2003). Hybridization efficiency of the adhesive/dentin interface with wet bonding. *J Dent Res* **82**, 141-145.

WANG, Y., SPENCER, P. & WALKER, M.P. (2007). Chemical profile of adhesive/caries-affected dentin interfaces using Raman microspectroscopy. *J Biomed Mater Res A* **81,** 279-286.

WATSON, T.F., ATMEH, A.R., SAJINI, S., COOK, R.J. & FESTY, F. (2014). Present and future of glass-ionomers and calcium-silicate cements as bioactive materials in dentistry: biophotonics-based interfacial analyses in health and disease. *Dent Mater* **30**, 50-61.

ZAVGORODNIY, A.V., ROHANIZADEH, R., BULCOCK, S. & SWAIN, M.V. (2008). Ultrastructural observations and growth of occluding crystals in carious dentine. *Acta Biomater* **4**, 1427-1439.

TABLE TITLES

Table 1. Materials and chemicals used in this study and respective manufacturers, basic

formulation and mode of application.

Table 2. Table of cases with correspondence to figures numbers.

LEGEND OF FIGURES

Figure 1. CLSM images (reflexion/fluorescence) showing the interfacial characterization and micropermeability of the glass ionomer cement Ketac-Bond/sound dentin interface, without load cycling. A weak pattern of micropermeability within the dentinal tubules (t) (arrows) and at the Rhodamine B-labeled cement (c) (asterisk), but null pattern of micropermeability at the largely hybrid layer (hl) may be observed at Fig. 1A. It is also shown a band of richly dye-infiltrated dentin just beneath the interface, but this band was formed due to the acidic effect of the conditioner and specific cement. Rhodamine-B permeating from the pulp has also infiltrated this band, which diffused laterally through the affected tubular walls and mixed with the fluorescein, exhibiting a light spectral overlap (yellow) (pointers) in the emission of profile of both dyes (red and green). Wider fusiform-shaped cement tags (ct) underneath the cement layer, and funneling in some specific locations (f) characterize the cement-dentin interface (scale bar: 10 μm). In the CLSM image captured in fluorescence mode and imaged with fluorescein (1B), a discrete dye sorption throughout the dentinal tubules is detected. The presence of dye in the restorative material indicates the micropermeability of the interface (scale bar: 10 μm). It is also possible to observe a cement layer characterized by the presence of many cement tags (ct) when imaged with Rhodamine (1C), underneath the cement layer (scale bar: 10 μm). This cement infiltration is also characterized by a moderate reflective signal inside the dentinal tubules, in the form of highly fluorescent structures (arrow) (1D) (scale bar: 10 μm). c, cement layer; d, dentin; ct, cement tags; f, funneling; hl, hybrid layer; t, dentinal tubules.

Figure 2. CLSM single-projection images disclosing the fluorescent calcium-chelator dye XO of the glass ionomer cement Ketac-Bond/sound dentin interface, without load cycling (2A) (scale bar: 10 μm). Interfacial characterization of the cement-dentin

interface, imaged with Rhodamine (2B) (scale bar: 10 μm) and calcium-chelator dye XO only (2C) (scale bar: 10 μm) are shown. Scarce and medium-size cement tags (arrows), below a very thin hybrid layer (pointers), are detected. Dentinal tubules and some extent of the hybrid layer appeared clearly stained with XO-dye, which showed a remarkable fluorescence signal due to consistent presence of Ca-minerals within the tubules (asterisk) and walls of dentinal tubules (double arrows).

Figure 3. CLSM images (reflexion/fluorescence) showing the interfacial characterization and micropermeability of the glass ionomer cement Ketac-Bond/sound dentin interface, after load cycling (3A) (scale bar: 10μm). Weaker signs of nanoleakage are characterized at this projection, where both scarce penetration of fluoroscein throughout the dentinal tubules (arrows) and water sorption within the thickness of the hybrid layer (hl) (asterisk) can be seen. A clear spectral overlap, at the hybrid layer (yellow-orange) in the emission of profile of both dyes (red, and green in lower proportion) characterizes the cement-dentin interface. A moderate reflective signal inside the dentinal tubules, indicating the presence of mineral components (pointers) are adverted. Longer and wider cement tags (ct) are detected. In the CLSM image captured in fluorescence, it is possible to observe a cement-dentin interface characterized by clear and continuous dye sorption throughout their thickness (arrows) (3B) (scale bar: 10 μm), and by the presence of multiple and non-regular-shaped cement tags (ct) when imaged with Rhodamine (3C) (asterisk) (scale bar: 10 μm). This cement-dentin infiltration is also characterized by a discrete reflective signal inside the dentinal tubules (t) (3D) (pointer) (scale bar: 10 μm). c, cement layer; d, dentin; ct, cement tags; hl, hybrid layer; t, dentinal tubules.

Figure 4. CLSM single projection image disclosing the fluorescent calcium-chelator dye XO of the resin-dentin interface created with glass ionomer cement Ketac-

Bond/sound dentin interface, after load cycling (4A) (scale bar: 10 μm). Interfacial characterization of the cement-dentin interface imaged with Rhodamine (4B) (scale bar: 10 μm) and calcium-chelator dye XO solely (4C) exhibits multiple intact cement tags imaged with Rhodamine (arrows), and mineral deposition at the interface, especially concentrated within the body of the material immediately adjacent to the dentin and along the walls of dentinal tubules (t) (arrows) (scale bar: 10 μm). t, dentinal tubules.

Figure 5. CLSM images (reflexion/fluorescence) showing the interfacial characterization and micropermeability of the glass ionomer cement Ketac-Bond/caries-affected dentin interface, without load cycling. A clear presence of micropermeability is exhibited between the cement (c) and the carious-affected dentin (d) interface, especially located within the body of the material immediately adjacent to the subjacent dentin (arrows). This permeability does not affect the walls of dentinal tubules, at Fig. 5A (scale bar: 10 μm). This interface shows a remarkable spectral overlap (yellow) (pointers) in the emission of profile of both dyes (red and green), and wider funnel-shaped cement tags (ct) underneath the cement layer. Thereby, the hybrid layer (hl) reveals a lack of sealing due to a tight dye sorption throughout its thickness, as is observed in the CLSM image captured in fluorescence mode and imaged with fluorescein (arrows). This dye sorption is extremely reduced throughout the *canaliculi* lumens (asterisk) (5B) (scale bar: 10 μm). The cement layer is characterized by the presence of abundant and robust cement tags (ct) when imaged with Rhodamine (5C) (scale bar: 10 μm). A weak reflective signal may provide a description from the bottom of the interface and inside the dentinal tubules (pointers), in the form of weakly fluorescent structures (5D) (scale bar: 10 μm). c, cement layer; d, dentin; hl, hybrid layer; ct, cement tags.

Figure 6. CLSM single-projection images disclosing the fluorescent calcium-chelator dye XO of the glass ionomer cement Ketac-Bond/caries-affected dentin interface, without load cycling (6A) (scale bar: 25 μm). The adhesive cement layer is characterized by the presence of multiple and discontinuous funnel-shaped cement tags (pointers), when imaged with Rhodamine (6B) (scale bar: 25 μm). Moderate fluorescence signal of XO-dye within an evident hybrid layer (hl), but strong within some dentinal tubules (t) (arrows), revealed the presence of calcium complexes within both adhesive structures (6C) (scale bar: 25 μm). ct, cement tags; hl, hybrid layer; t, dentinal tubules.

Figure 7. CLSM images (reflexion/fluorescence) showing the interfacial characterization and micropermeability of the glass ionomer cement Ketac-Bond/caries-affected dentin interface, after load cycling (7A) (scale bar: 10μm). The cement-dentin interface imaged in reflexion/fluorescence shows some both absence signs of nanoleakage and water sorption (pointer) and a moderate reflective signal from inside the dentinal tubules, indicating the presence of mineral components (arrows). A very limited dye diffuses into the adhesive cement layer (c), when imaged in Rhodamine (7B), but localized tubular micropermeability was detected at some tubule (t), below the deposit of mineral (faced arrows), as scarce penetration of fluoroscein throughout the dentinal tubules is confirmed (scale bar: 10 μm). Longer and funnel-shaped cement tags are also detected at the interface (ct) (7C) (scale bar: 10 μm). This cement-dentin interface is also characterized by a moderate reflective signal inside the dentinal tubules (7D) (scale bar: 10 μm) (arrow). d, dentin; c, cement layer; ct, cement tags; hl, hybrid layer; t, dentinal tubules.

Figure 8. CLSM single-projection images disclosing the fluorescent calcium-chelator dye XO of the glass ionomer cement Ketac-Bond/caries-affected dentin interface, after

load cycling (8A) (scale bar: 10 μm). Xo-dye penetrates, in general, the first 5-10 μm of cement tags (arrow), and longer extent, occasionally. The rest of cement tags-length appeared with the characteristic Rhodhamine B-labeled colorant (pointers), when imaged in Rhodamine only (8B) (scale bar: 10 μm). A clear fluorescence signal due to consistent presence of xylenol-stained Ca-deposits within the hybrid layer (hl), walls of dentinal tubules (dt) and cement tags (ct) were observed with calcium-chelator dye Xo solely (8C) (scale bar: 10 μm). hl, hybrid layer; t, cement tags; t, dentinal tubules.

Figure 9. CLSM images (reflexion/fluorescence) showing the interfacial characterization and micropermeability of the resin-modified glass ionomer cement Vitrebond Plus/sound dentin interface, without load cycling. A very weak pattern of water sorption within the Rhodamine B-labeled cement (c), is detectable (9A), exhibiting a light spectral overlap (yellow) in the emission of profile of both dyes (red and green), within the body of the material (asterisk). Any nanoleakage signal from the hybrid layer (hl) located underneath the adhesive cement layer may be observed (scale bar: 10 μm). In the CLSM image captured in fluorescence, it is possible to notice an adhesive cement layer characterized by the absence of cement tags (9C) (scale bar: 10 μm) when imaged with Rhodamine and by a faint dye sorption throughout their thickness (9B) (scale bar: 10 μm) (asterisk). This resin-modified glass ionomer cement infiltration is also characterized by an indiscernible reflective signal inside the dentinal tubules, in the form of faintly fluorescent structures (9D) (scale bar: 10 μm). hl, hybrid layer; d, dentin; c, cement layer.

Figure 10. Confocal microscopy evaluation (CLSM) single-projection images disclosing the fluorescent calcium-chelator dye XO of the glass ionomer cement Vitrebond Plus/sound dentin interface, without load cycling (10A) (scale bar:10 μm). The adhesive cement layer is characterized by the presence of an intensive intertubular

cement infiltration, with prominent and continuous primary and secondary cement tags (ct), when imaged with Rhodamine (10B) (scale bar: 10 μm). Weak fluorescence signal of XO-dye within the hybrid layer (hl), but null signal of XO-dye within the dentinal tubules (t), except in someone occasional tubule (arrow), revealed the generalized lack of calcium complexes within both adhesive structures (10C) (scale bar: 10 μm). hl, hybrid layer; c, cement; ct, cement tags; d, dentin; t, dentinal tubules.

Figure 11. CLSM images (reflexion/fluorescence) showing the interfacial characterization and micropermeability of the resin-modified glass ionomer cement Vitrebond Plus/sound dentin interface, after load cycling (11A) (scale bar: 10μm). A richly dye-infiltrated band flooded by fluorophores leaching from the cement (faced arrows) is detected. A weaker nanoleakage signal from the hybrid layer (pointers) (hl) located underneath the body of the material layer, may be pointed out. A faint spectral overlap (yellowish) in the emission of profile of both dyes (red and green), corresponds with clear signs of nanoleakage, and dye-deficient zones are also seen within this area (double arrows), representing the unaffected peritubular dentin. The adhesive cement layer (c) is characterized by strong dye sorption throughout its entire thickness (asterisks) (11B) (scale bar: 10 μm), and by the presence of medium-length cylindrical cement tags (ct) (11C) (scale bar: 10 μm). This cement-dentin infiltration is also characterized by a potent reflective signal inside the dentinal tubules (t), in the form of globular appearance (11D) (arrows) (scale bar: 10 μm). hl, hybrid layer; c, cement layer; d, dentin; ct, cement tags; t, dentinal tubules.

Figure 12. CLSM single projection image disclosing the fluorescent calcium-chelator dye XO of the resin-dentin interface created with resin-modified glass ionomer cement Vitrebond Plus/sound dentin interface, after load cycling 12A) (scale bar: 10 μm). Interfacial characterization of the cement (c)-dentin (d) interface imaged with

Rhodamine (12B) (scale bar: 10 μm) and calcium-chelator dye XO only (12C) (scale bar: 10 μm). A modest fluorescence signal due to consistent presence of xylenol-stained Ca-deposits within the hybrid layer (hl), walls of dentinal tubules (t) (arrows) and within the cement tags (ct) (pointers) are unveiled. Note the presence of intact resin tags imaged in Rhodamine excitation/emission mode (faced arrows). hl, hybrid layer; c, cement layer; d, dentin; ct, cement tags; t, dentinal tubules.

Figure 13. CLSM images (reflexion/fluorescence) showing the interfacial characterization and micropermeability of the resin-modified glass ionomer cement Vitrebond Plus/caries-affected dentin interface, without load cycling. Figure 13A shows a generalized pattern of absent micropermeability and water sorption (arrows) at the Rhodamine B-labeled adhesive cement layer (c), but present at the dentinal tubules (t) (arrows) (scale bar: 25 μm). In the CLSM image captured in fluorescence mode, it is possible to observe an adhesive cement layer characterized by the presence of many incipient, thin and short cement tags (rt) when imaged with Rhodamine (13C) underneath the adhesive cement layer without dye uptake by the restoration when imaged with fluorescein (asterisk) (13B). Faint reflective signals may be described from the bottom of the interface and inside the dentinal tubules (pointers) (13D) (B, C, D, scale bar: 25 μm). c, cement layer; ct, cement tags. t, dentinal tubules.

Figure 14. CLSM single-projection images disclosing the fluorescent calcium-chelator dye XO of the resin-modified glass ionomer cement Vitrebond Plus/caries-affected dentin interface, without load cycling (14A) (scale bar: 10 μm). Signals of xylenol orange stain are observed at the top of cement-dentin interface (pointers), and at the walls of the dentinal tubules (arrows). 14B exhibits multiple, intact and long cement tags (ct) imaged with Rhodamine, demonstrating adequate penetration of the resin-modified glass ionomer cement into the caries-affected dentin thickness (scale bar: 10

μm). The hybrid layer (hl) and the tubular dentin (dt) walls stained with fluorescent calcium-chelator dye XO (14C) (scale bar: 10 μm), evidencing the remineralization and sealing of the cement-dentin interface. hl, hybrid layer; ct, cement tags; d, dentin; t, dentinal tubules.

Figure 15. CLSM images (reflexion/fluorescence) showing the interfacial characterization and micropermeability of the rein-modified glass ionomer cement Vitrebond Plus/caries-affected dentin interface, after load cycling (15A), showing strong micropermeability between the Rhodamine B-labeled cement layer (c) and dentin (d) (arrow), specially localized at the bottom of the hybrid layer (hl). A spread dentin porosity and evident nanoleakage signals from the absorption layer located below the labeled adhesive cement layer and infiltrated throughout the intertubular dentin. Severe dye uptake throughout its thickness is noted (asterisk) (scale bar: 10μm). Fluoroscein dye results accumulated at the interior of tubules (dt) (pointers) (15B) (scale bar: 10 μm). In the CLSM image captured in fluorescence mode, it is possible to observe an adhesive cement layer characterized by the presence of some shorter cement tags (ct) (15C) (scale bar: 10 μm), when imaged with Rhodamine mode only. Poor reflective signal inside the dentinal tubules is detected (faced arrows) (15D) (scale bar: 10 μm), indicating the presence of some mineral components. hl, hybrid layer; ct, cement tags; t, dentinal tubules.

Figure 16. CLSM single-projection images disclosing the fluorescent calcium-chelator dye XO of the resin-modified glass ionomer cement Vitrebond Plus/caries-affected dentin interface, after load cycling (16A). Signals of xylenol orange stain are observed within the cement-infiltrated intertubular dentin (arrows), and at the entrance of the dentinal tubules (t), in combination with the cement tags (pointers). When imaged with Rhodamine mode solely, funnel-shaped and longer cement tags (ct), reproducing the

tubules profile of the demineralized carious peritubular dentin, are observed (scale bar: 10 μm). Multiple secondary cement tags, demonstrating adequate penetration of the resin-modified glass ionomer cement into the caries-affected dentin thickness, were also detected (faced arrows) (16B) (scale bar: 10 μm). The infiltrated intertubular dentin and the peritubular dentin (dt) walls stained with fluorescent calcium-chelator dye XO (16C) (scale bar: 10 μm), evidencing remineralization at the cement-dentin interface. ct, cement tags; d, dentin; dt, dentinal tubules.
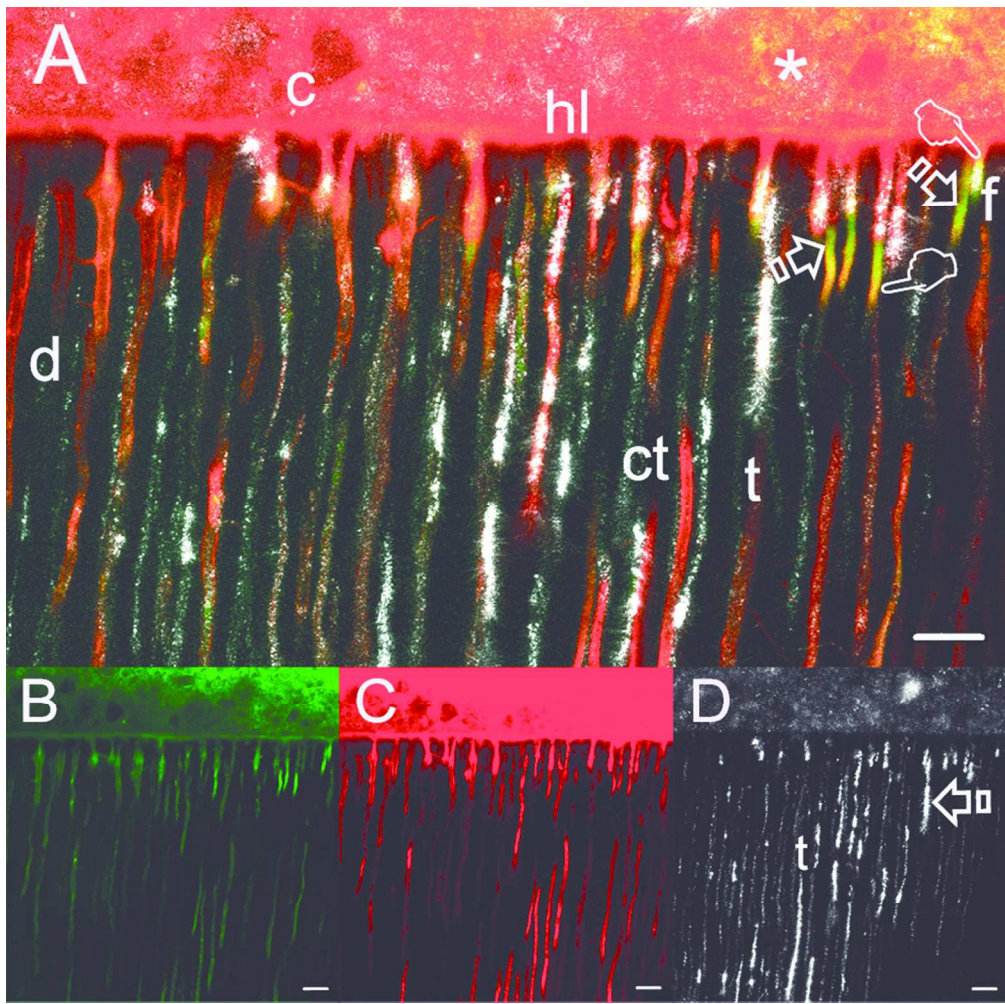
Figure 1

83x83mm (300 x 300 DPI)
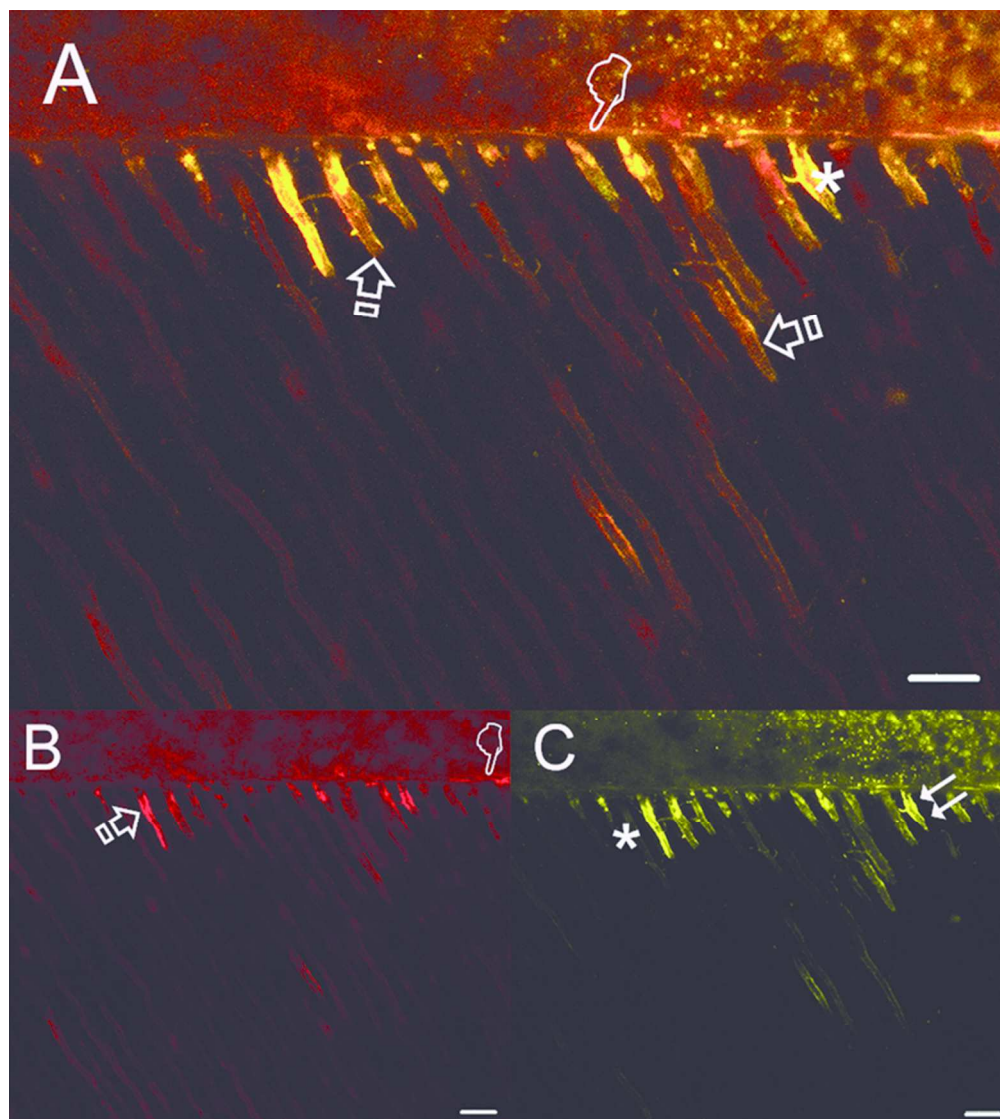
Figure 2

83x93mm (300 x 300 DPI)
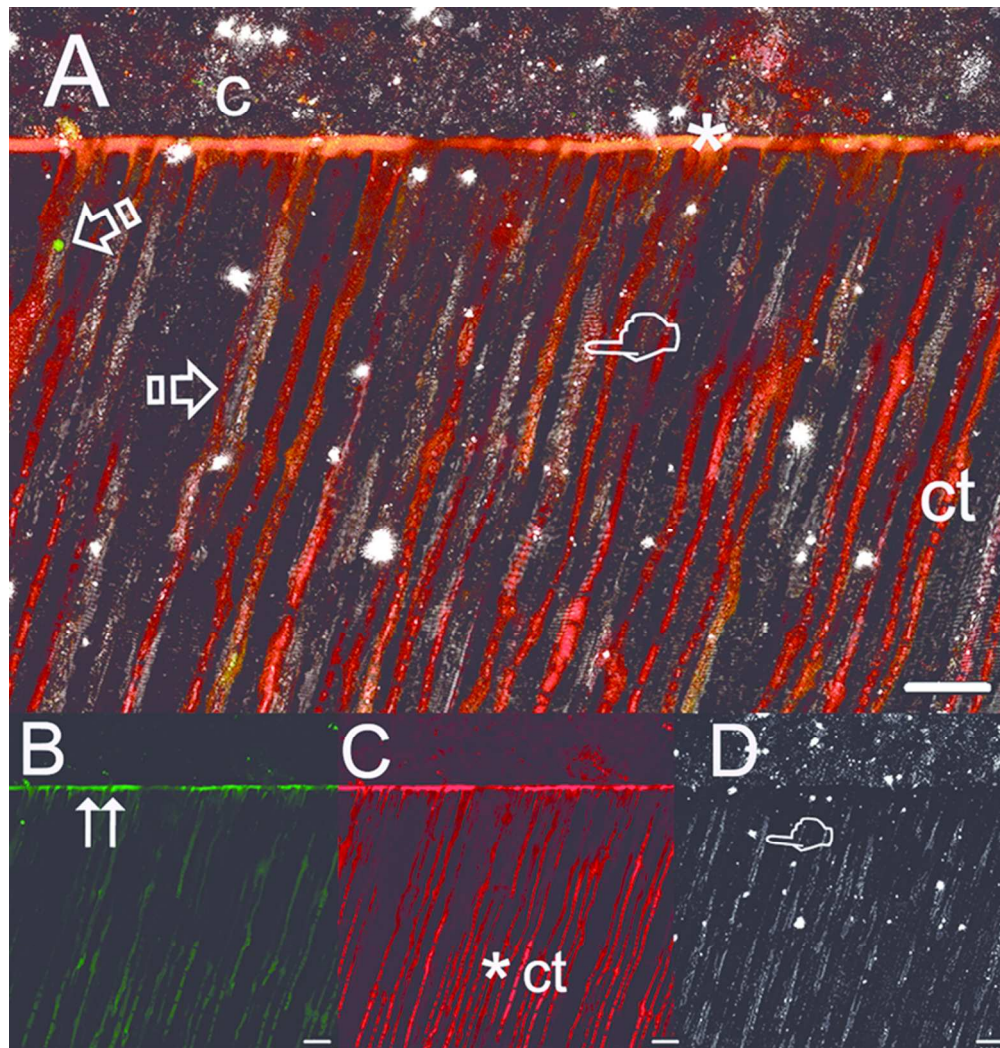
Figure 3

83x87mm (300 x 300 DPI)
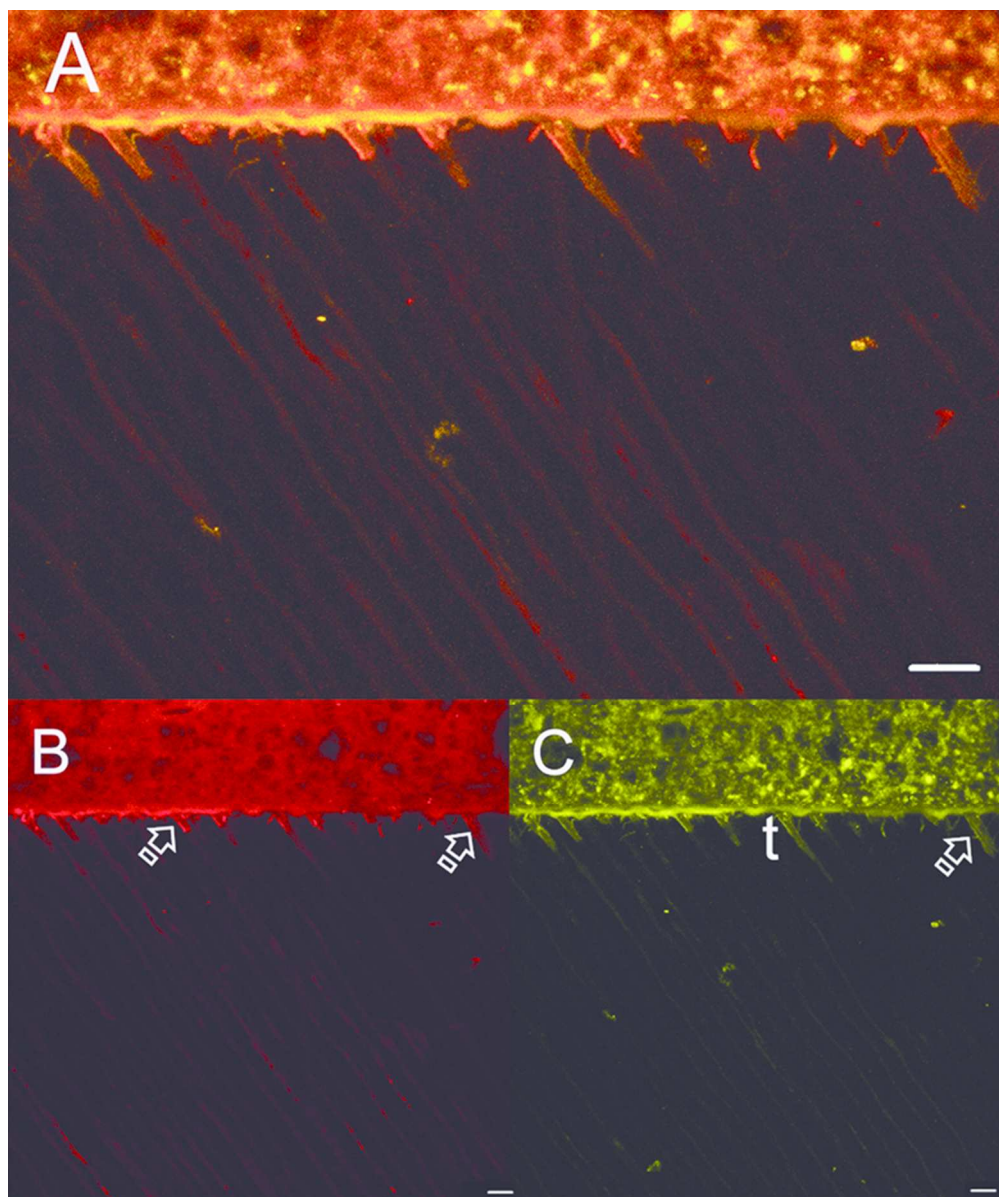
Figure 4

83x99mm (300 x 300 DPI)
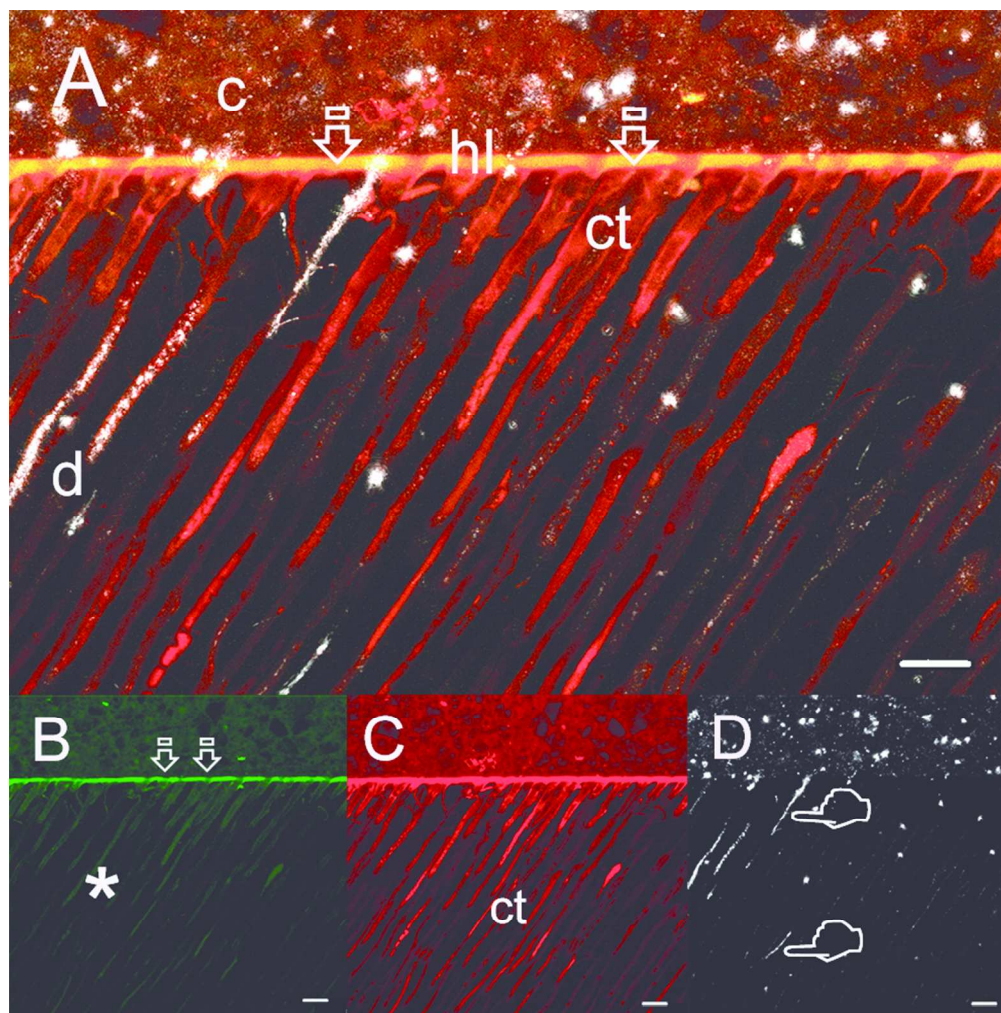
Figure 5

83x84mm (300 x 300 DPI)
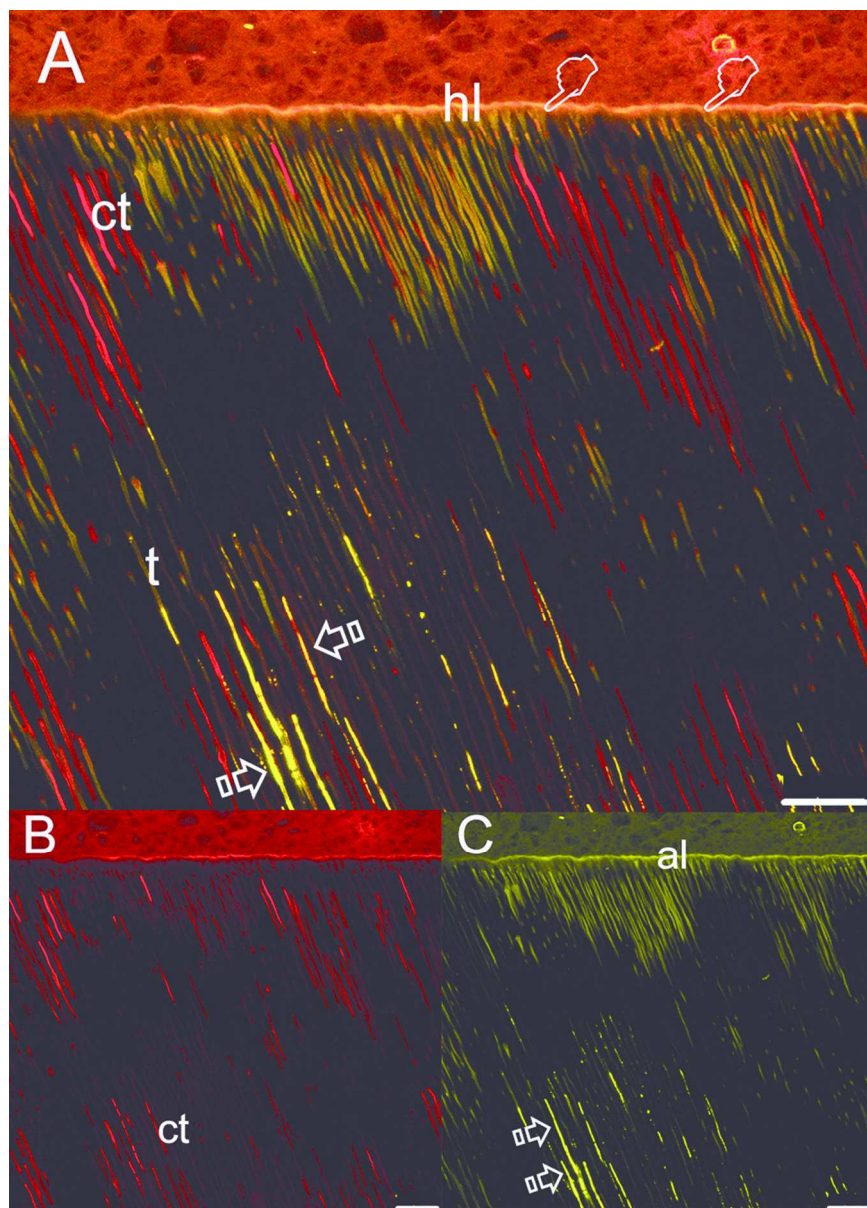
Figure 6

83x115mm (300 x 300 DPI)
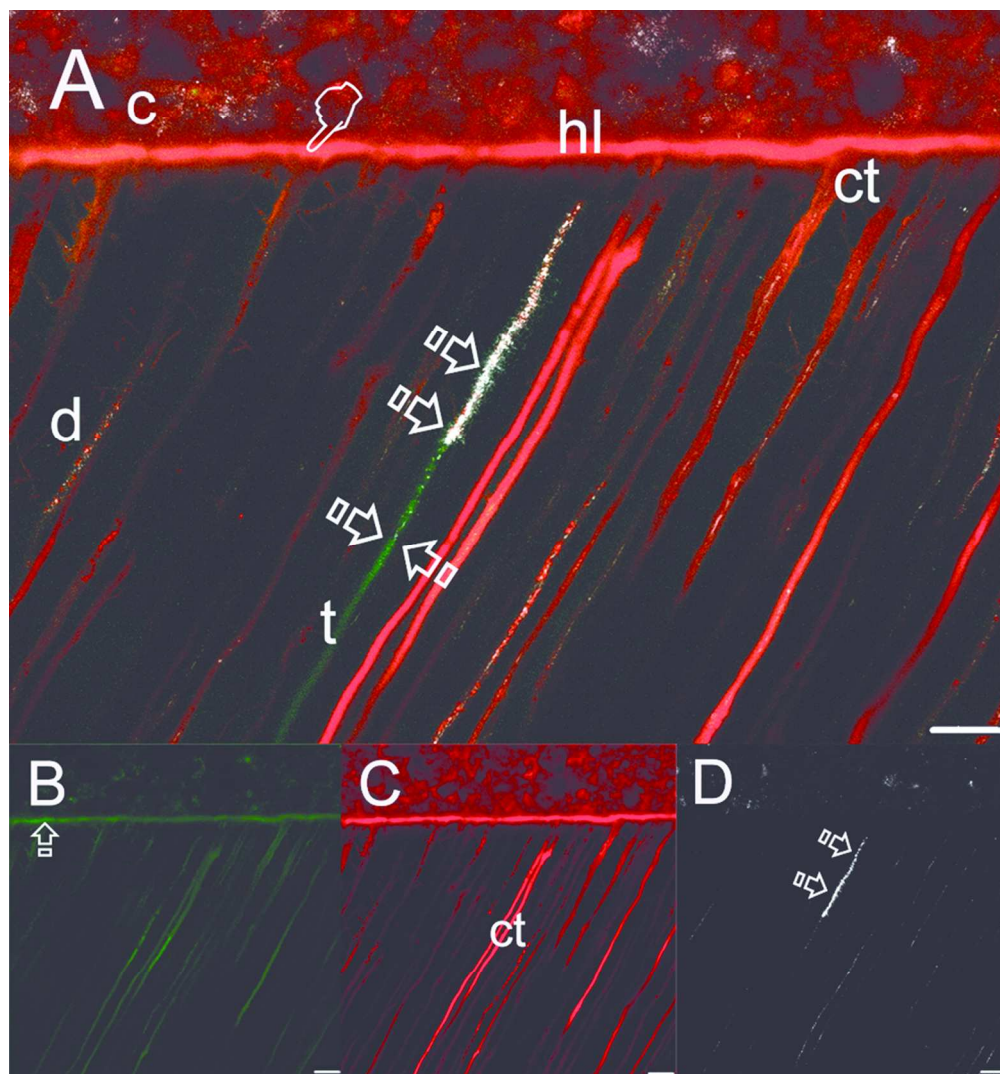
Figure 7

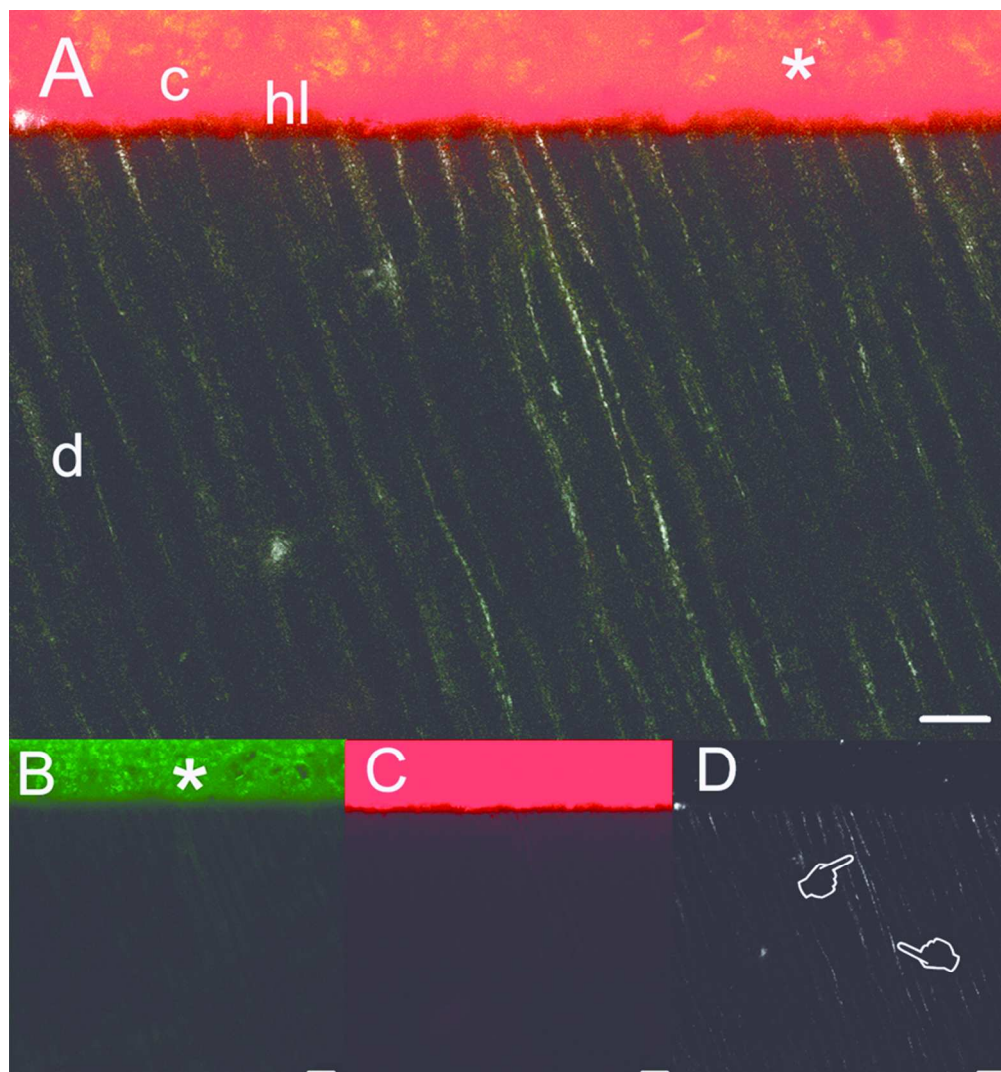83x89mm (300 x 300 DPI)
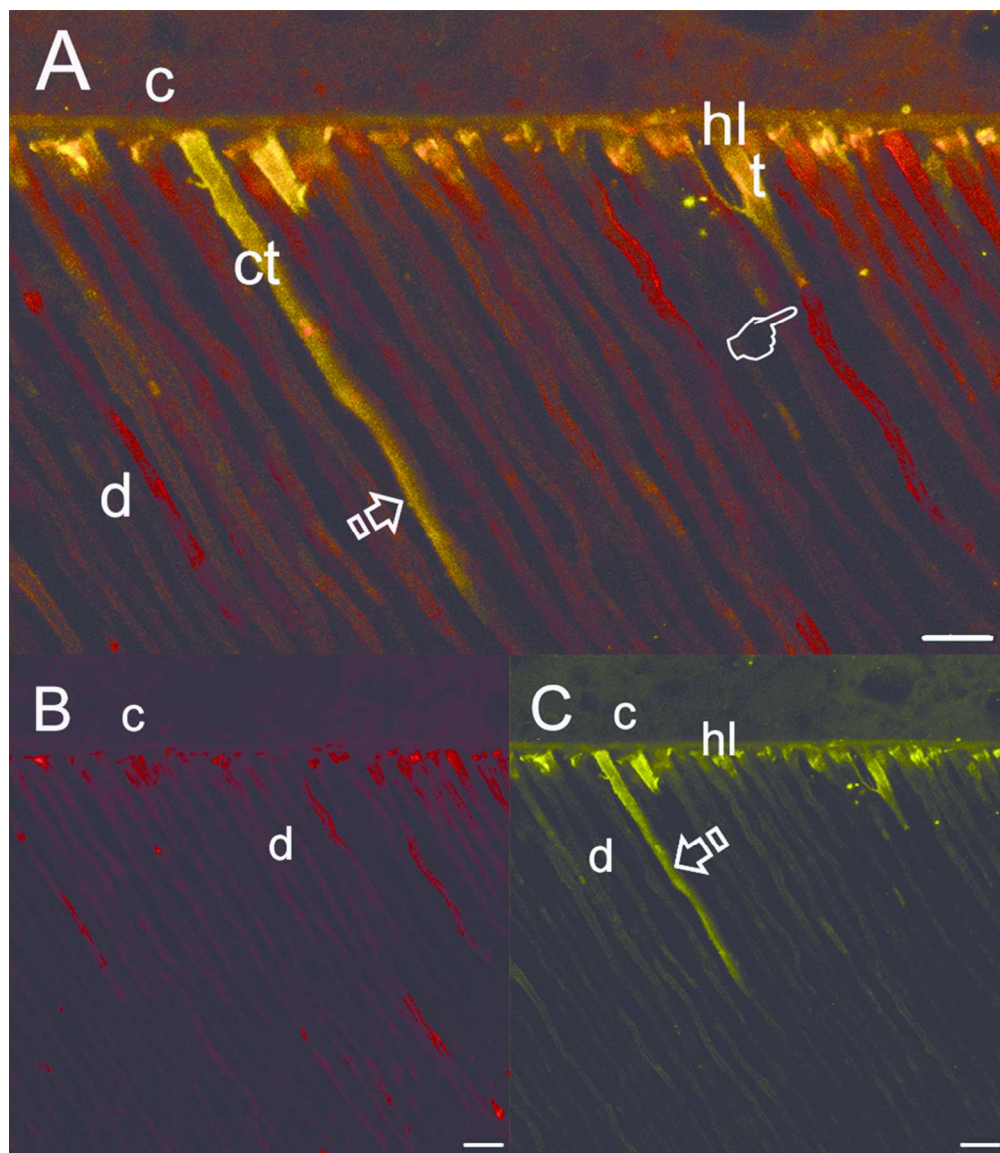
Figure 8

84x96mm (300 x 300 DPI)

Figure 9
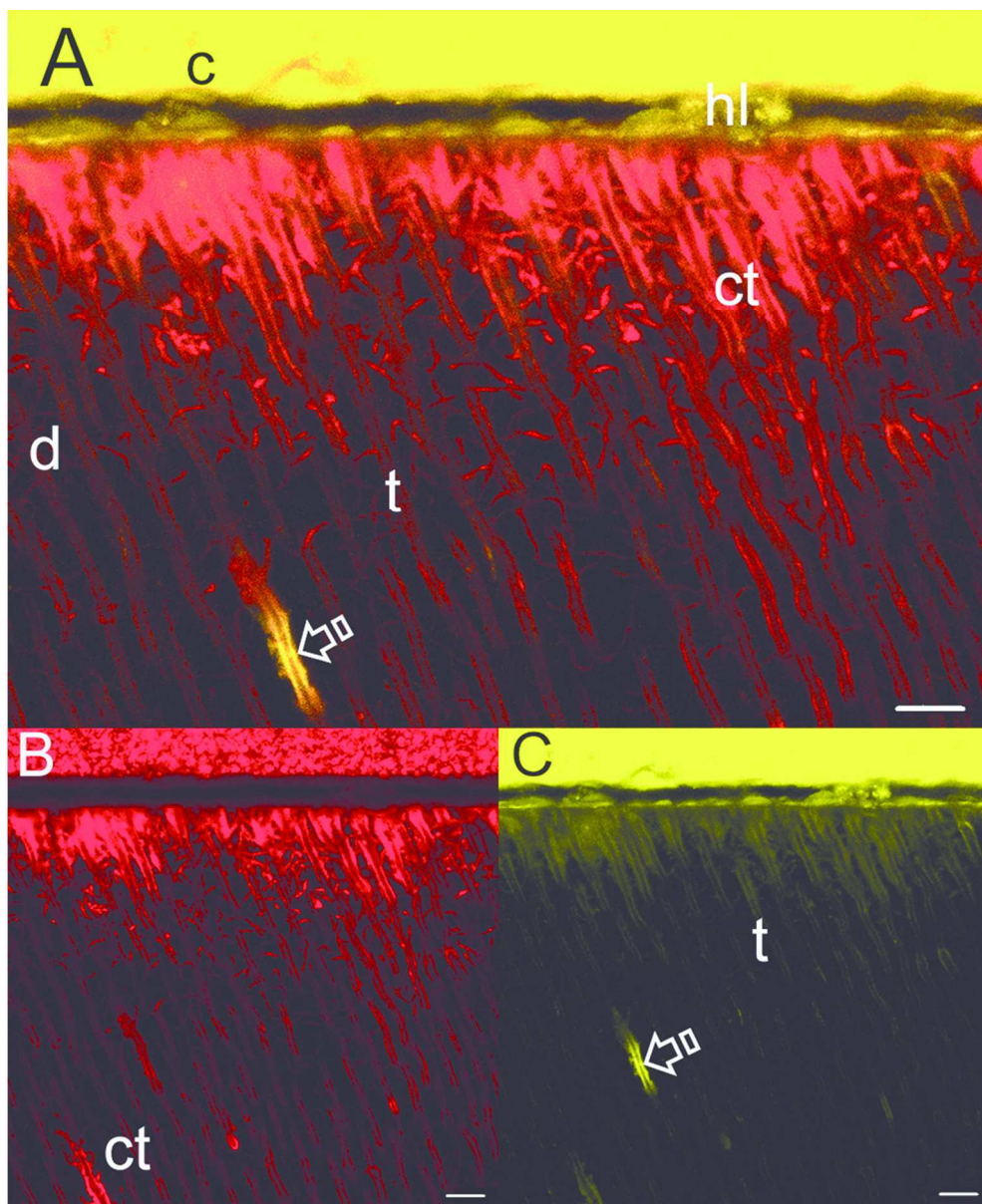
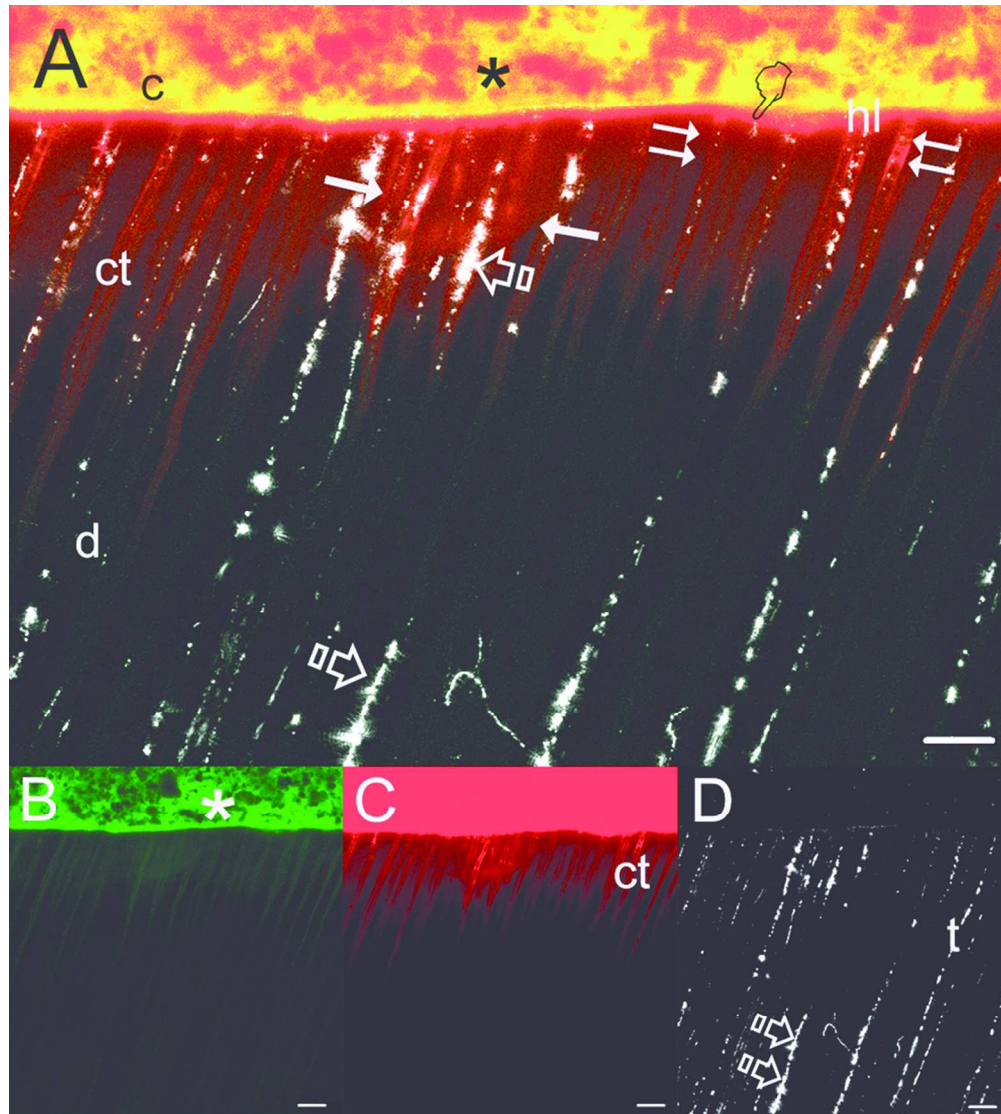83x89mm (300 x 300 DPI)

Figure 10

83x102mm (300 x 300 DPI)

Figure 11
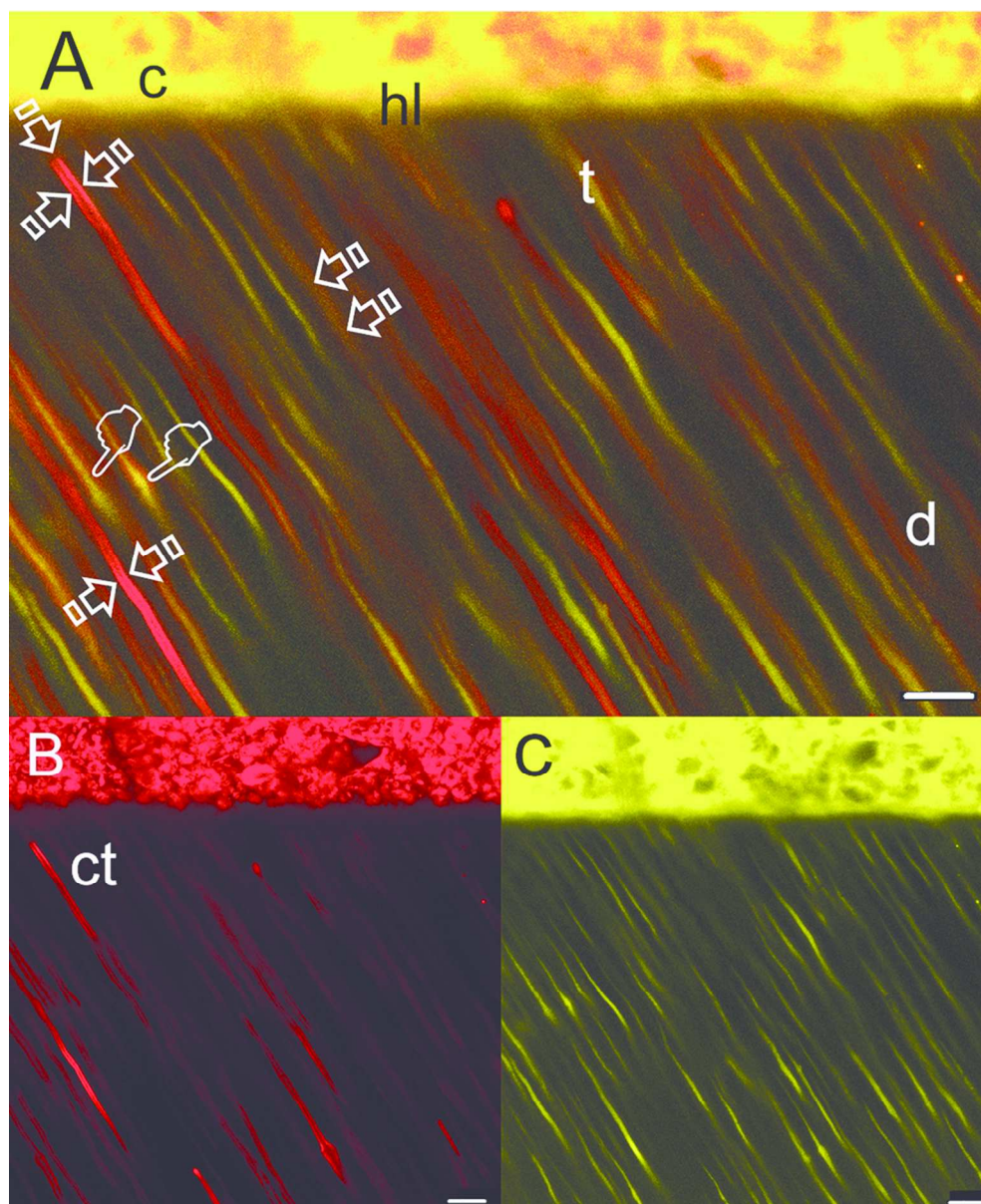
83x93mm (300 x 300 DPI)

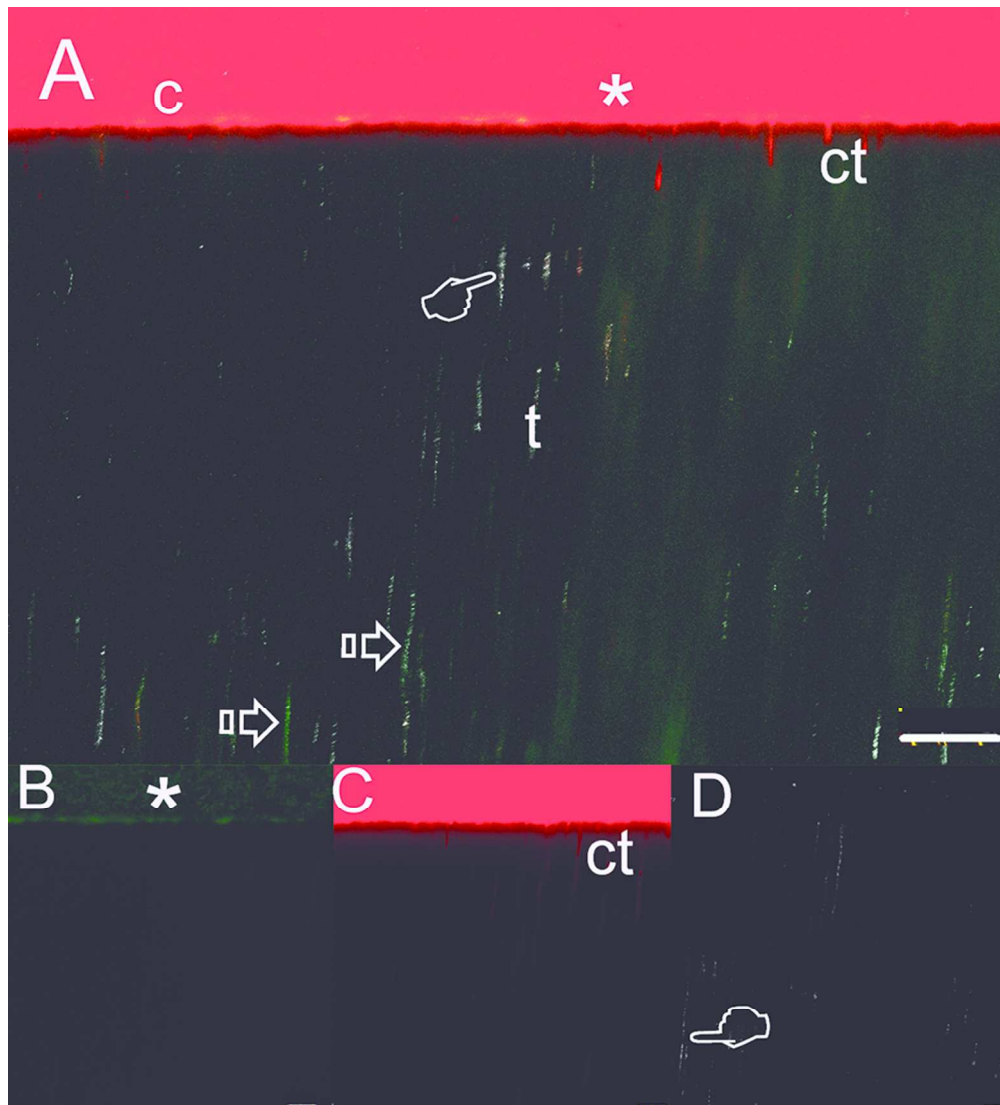Figure 12

83x102mm (300 x 300 DPI)

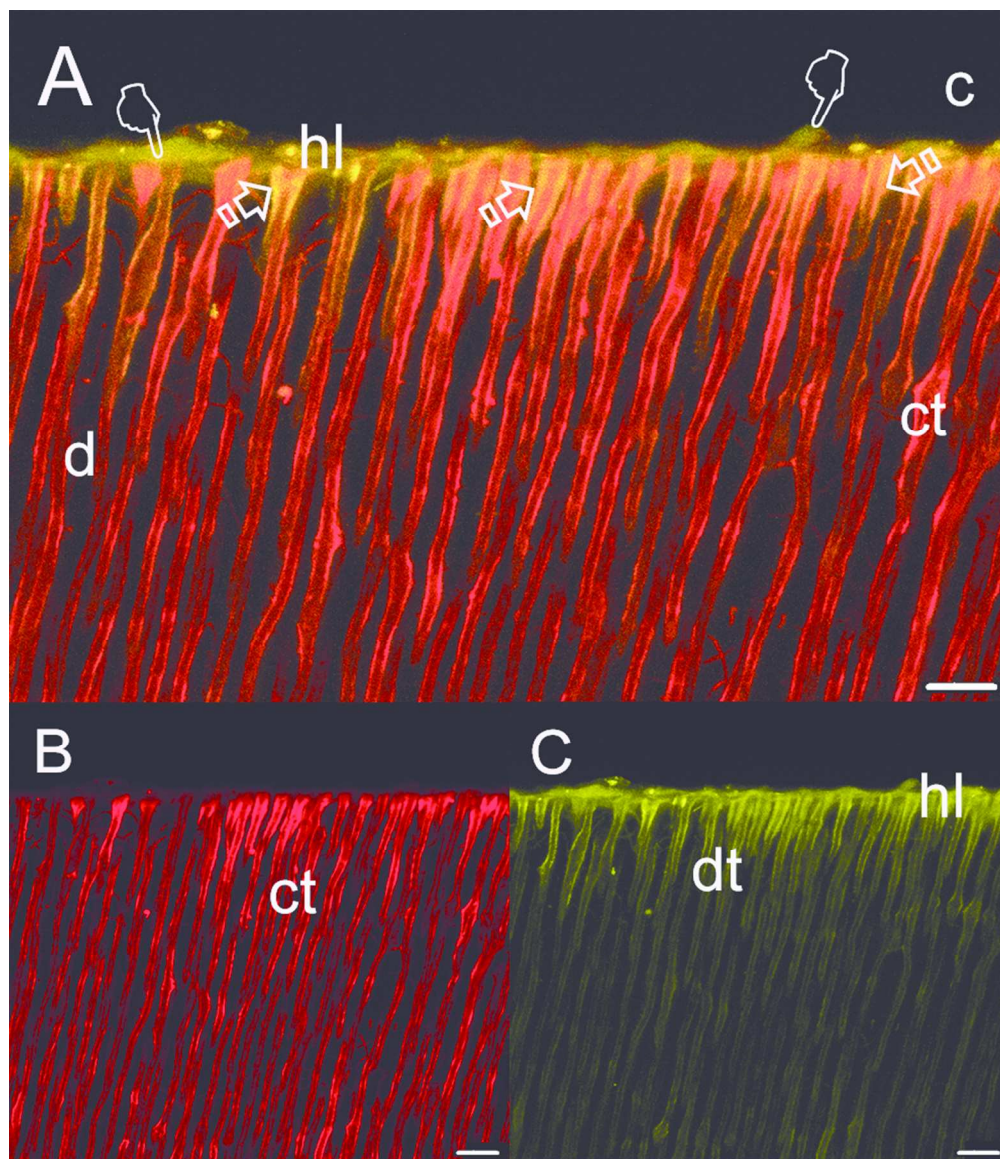Figure 13

83x92mm (300 x 300 DPI)

Figure 14
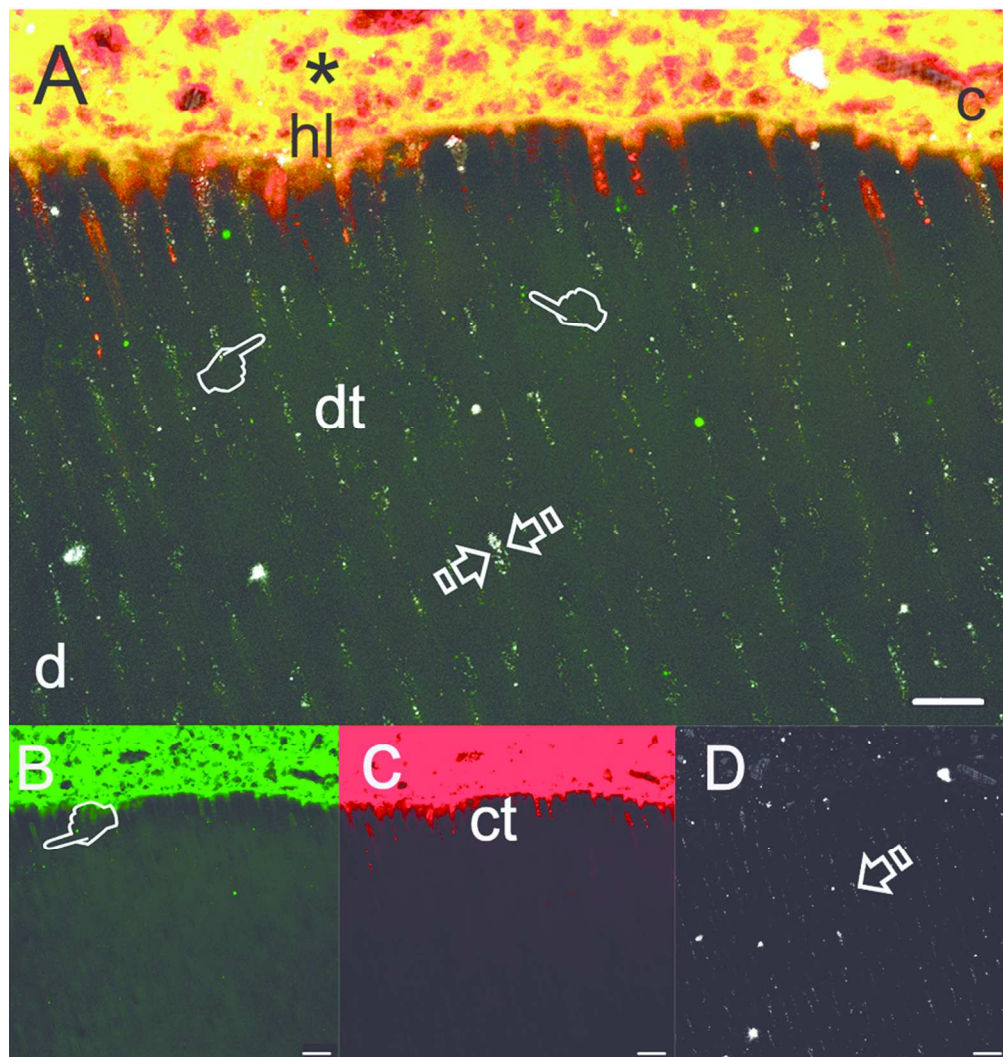
83x96mm (300 x 300 DPI)

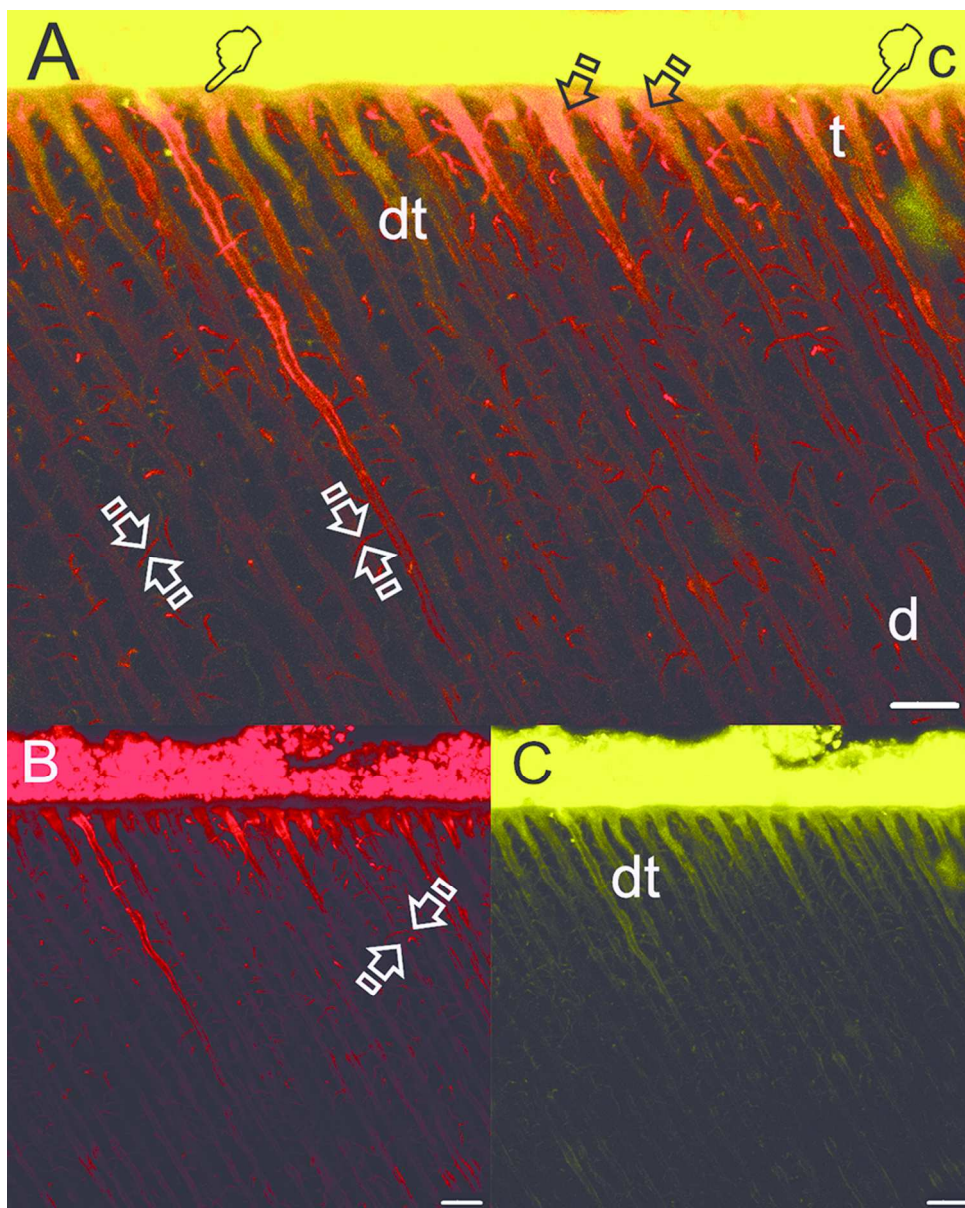Figure 15

83x88mm (300 x 300 DPI)

Figure 16

83x104mm (300 x 300 DPI)

Table 1. Materials and chemicals used in this study and respective manufacturers, basic

formulation and mode of application

Product details	Basic formulation	Mode of application
Ketac Bond (3M Deustchland GmbH, Neuss, Germany)	***Ketac conditioner:*** polycarboxylic (25% polyacrylic) acid, water (75%) ***Powder:*** calcium-aluminum-lanthanium-fluorosilica glass, pigments. ***Liquid:*** polycarboxylic acid, tartaric acid, water, conservation agents.	- Apply Ketac conditioner (10 s) - Rinse with water. - Mix powder and liquid components. - Apply.
Vitrebond Plus (3M Deustchland GmbH, Neuss, Germany)	***Liquid:*** resin-modified polyalkenoic acid, HEMA, water, initiators. ***Paste:*** HEMA, Bis-GMA, water, initiators and radiopaque FAS.	- Mix paste/liquid components (10-15s). - Apply. - Light activation (20s).
X-Flow^{TM} (Dentsply, Caulk, UK)	Strontium alumino sodium fluorophosphorsilicate glass, di- and multifunctional acrylate and methacrylate resins, DGDMA, highly dispersed silicon dioxide UV stabilizer, ethyl-4-dimethylaminobenzoate camphorquinone, BHT, iron pigments, titanium dioxide.	
SBFS (pH=7.45)		
Sigma Aldrich, St. Louis, MO, USA	NaCl 8.035 g NaHCO$_3$ 0.355 g K$_2$HPO$_4$·3H$_2$O 0.231 g, MgCl$_2$·6H$_2$O 0.311 g 1.0 M – HCl 39 ml Tris 6.118 g	
Panreac Química SA, Barcelona, Spain	KCl 0.225 g CaCl$_2$ 0.292 g Na$_2$SO$_4$ 0.072 g 1.0 M – HCl 0–5 ml	

Abbreviations: HEMA: 2-hydroxyethyl methacrylate; Bis-GMA: bisphenol A diglycidyl methacrylate; FAS: fluoraluminosilicate; DGDMA: diethyleneglycol dimethacrylate phosphate; BHT: butylated hydroxytoluene; SBFS: simulated body fluid solution; NaCl: sodium chloride; NaHCO$_3$: sodium bicarbonate; KCl: potassium chloride; K$_2$HPO$_4$·3H$_2$O: potassium phosphate dibasic trihydrate; MgCl$_2$·6H$_2$O: magnesium chloride hexahydrate; HCl: hydrogen chloride; CaCl$_2$: Calcium chloride; Na$_2$SO$_4$: sodium sulfate; Tris: tris(hydroxylmethyl) aminomethane.

1

Table 2. Table of cases with correspondence to figures numbers.

Figure number	Dentin	Dentin pre-treatment	Glass ionomer-cement	Load	Dye
1	SD	Polyacrylic acid	Ketac-Bond	No	Rd/Fl
2	SD	Polyacrylic acid	Ketac-Bond	No	Rd/Xo
3	SD	Polyacrylic acid	Ketac-Bond	Yes	Rd/Fl
4	SD	Polyacrylic acid	Ketac-Bond	Yes	Rd/Xo
5	CAD	Polyacrylic acid	Ketac-Bond	No	Rd/Fl
6	CAD	Polyacrylic acid	Ketac-Bond	No	Rd/Xo
7	CAD	Polyacrylic acid	Ketac-Bond	Yes	Rd/Fl
8	CAD	Polyacrylic acid	Ketac-Bond	Yes	Rd/Xo
9	SD	None	Vitrebond Plus	No	Rd/Fl
10	SD	None	Vitrebond Plus	No	Rd/Xo
11	SD	None	Vitrebond Plus	Yes	Rd/Fl
12	SD	None	Vitrebond Plus	Yes	Rd/Xo
13	CAD	None	Vitrebond Plus	No	Rd/Fl
14	CAD	None	Vitrebond Plus	No	Rd/Xo
15	CAD	None	Vitrebond Plus	Yes	Rd/Fl
16	CAD	None	Vitrebond Plus	Yes	Rd/Xo

Abreviations: Rd: Rhodamine B; Fl: fluorescein; Xo: Xylenol orange; SD: sound dentin; CAD: caries-affected dentin.